

Copyright © by SIAM. Unauthorized reproduction of this article is prohibited.

DOI:

<https://doi.org/10.1137/20M1382520>

Access to this work was provided by the University of Maryland, Baltimore County (UMBC) ScholarWorks@UMBC digital repository on the Maryland Shared Open Access (MD-SOAR) platform.

Please provide feedback

Please support the ScholarWorks@UMBC repository by emailing scholarworks-group@umbc.edu and telling us what having access to this work means to you and why it's important to you. Thank you.

MULTILAYERED POROELASTICITY INTERACTING WITH STOKES FLOW*

LORENA BOCIU[†], SUNČICA CANIC[‡], BORIS MUHA[§], AND JUSTIN T. WEBSTER[¶]

Abstract. We consider the interaction between an incompressible, viscous fluid modeled by the dynamic Stokes equation and a multilayered poroelastic structure which consists of a thin, linear, poroelastic plate layer (in direct contact with the free Stokes flow) and a thick Biot layer. The fluid flow and the elastodynamics of the multilayered poroelastic structure are fully coupled across a fixed interface through physical coupling conditions (including the Beavers–Joseph–Saffman condition), which present mathematical challenges related to the regularity of associated velocity traces. We prove the existence of weak solutions to this fluid-structure interaction problem with either (i) a linear, dynamic Biot model or (ii) a nonlinear quasi-static Biot component, where the permeability is a nonlinear function of the fluid content (as motivated by biological applications). The proof is based on constructing approximate solutions through Rothe’s method and using energy methods and a version of the Aubin–Lions compactness lemma (in the nonlinear case) to recover the weak solution as the limit of approximate subsequences. We also provide uniqueness criteria and show that constructed weak solutions are indeed strong solutions to the coupled problem if one assumes additional regularity.

Key words. poroelasticity, fluid-poroelastic structure interaction, poroelastic plate, multilayered poroelasticity, well-posedness

AMS subject classifications. 74F10, 76S05, 74L15, 34A01, 74K20

DOI. 10.1137/20M1382520

1. Introduction and literature review. Poroelasticity refers to fluid flow, as described by Darcy’s law, within deformable, porous media. Historically, studies of the fluid flow through porous media were motivated by applications in geosciences (see, e.g., [27]). The classic partial differential equation (PDE) model for such flows, based on consolidation theory, was originally introduced by Biot [10, 11, 12] and predicated upon phenomenological modeling. An alternative approach considers the fluid-structure interaction system at the level of the pores, with a derivation of an effective model based on homogenization techniques (see [3, 30, 38] and the references therein). Derivation of poroelastic models based on a continuum mechanics approach can be found in the monograph of Coussy [25]. Recently, Mikelić and

*Received by the editors November 25, 2020; accepted for publication (in revised form) August 13, 2021; published electronically November 1, 2021.

<https://doi.org/10.1137/20M1382520>

Funding: The work of the first author was partially supported by the National Science Foundation grant DMS-1555062 (CAREER). The work of the second author was partially supported by National Science Foundation grants DMS-1853340, DMS-2011319. The work of the third author was partially supported by the Croatian Science Foundation project IP-2019-04-1140. The work of the fourth author was partially supported by National Science Foundation grant DMS-1907620. The work of the third and fourth authors was also supported by the UMBC’s Office of Research Development through a SURFF grant, as well as the Department of Mathematics and Statistics for facilitating their collaboration in October and November, 2020.

[†]Department of Mathematics, North Carolina State University, Raleigh, NC 27695 USA (lvbociu@ncsu.edu).

[‡]Department of Mathematics, University of California, Berkeley, Berkeley, CA 94720 USA (canics@berkeley.edu).

[§]Department of Mathematics, Faculty of Science, University of Zagreb, 10000, Zagreb, Croatia (borism@math.hr).

[¶]Department of Mathematics and Statistics, University of Maryland, Baltimore County, Baltimore, MD 21250 USA (websterj@umbc.edu).

co-authors presented a mathematically rigorous derivation of lower-dimensional poroelastic models, such as poroelastic plates and shells, which can be found in [36]. From the point of view of PDE well-posedness, the classical Biot system has been extensively studied by many authors (see, e.g., [8, 9, 43, 47, 49, 51, 54]). Since poroelastic structures are ubiquitous in biological systems, recently there has been a growing interest in the analysis of poroelasticity in the context of biomedical applications (see, e.g., [6, 7, 14, 15, 17, 20, 23, 26, 32, 53] and the references and discussions therein).

In a variety of biomedical applications, the poroelastic structure is often in contact with a free fluid flow, such as, e.g., the blood flow through an artery with poroelastic walls. Mathematically, such problems are described by a coupled system of partial differential equations: the fluid equations (e.g., the Navier–Stokes or Stokes system) on one side, and the equations of poroelasticity on the other. These coupled problems are referred to as fluid-poroelastic structure interaction (FPSI) problems and have been analyzed, for instance, in [1, 24, 45, 46, 48]. However, many biological tissues (such as arterial walls), have a *multilayered structure*. In bioengineering, a multilayered poroelastic structure arises in the design of a bioartificial pancreas [50]. In bioartificial pancreas, healthy pancreatic cells are seeded in a poroelastic agarose or alginate gel, and the gel is encapsulated between two poroelastic plates, which are designed to exclude the patients own immune cells from attacking the organ while allowing passage of oxygen and nutrients to the pancreatic cells [50]. This multilayered poroelastic medium is connected to the blood flow via a tube (an anastomosis graft). The blood flows over the poroelastic plate and it passes into the poroelastic medium containing the transplanted cells, bringing oxygen and nutrient supply to the cells. Thus, the poroelastic plate in this design separates the poroelastic region containing the pancreatic cells on one side, from the region containing free blood flow on the other. One of the problems in this bioartificial pancreas design is to understand fluid (blood) flow through the poroelastic plate and poroelastic gel containing the cells, and simulate oxygen and nutrients supply to the cells.

Motivated by these types of applications, in the present paper we are interested in the mathematical aspects of the interaction between the flow of an incompressible, viscous fluid and a multilayered poroelastic structure. The multilayered poroelastic structure under consideration consists of two layers: a thin poroelastic layer in direct contact with the free fluid flow and a thick poroelastic layer sitting atop the thin layer (see Figure 1). The fluid flow is described by the time-dependent Stokes equations, while the thin and thick poroelastic layers are described by a poroelastic plate model and a Biot model, respectively. The three different physical models (the fluid model, the thin poroelastic structure model, and the thick Biot system) are fully coupled across a fixed interface by physically motivated interface conditions. We mention that interface conditions between porous media (Biot model(s)) and adjacent free fluid flow were rigorously analyzed in [34, 35]. Although slightly different from [34], our interface conditions involve a jump in the pressure between the free fluid and the Biot pressure at the interface. However, in contrast with the pressure jump derived in [34] through boundary layer considerations, the pressure jump in the present paper is a consequence of the presence of a thin poroelastic plate, which serves as the fluid-structure interface.

In the multilayered poroelastic structure, we consider two distinct scenarios: (i) a linear, dynamic Biot model or (ii) a nonlinear quasi-static Biot component where the permeability is a nonlinear function of the fluid content. The second case is motivated by biological applications [21, 23, 27, 33]. In particular, our main motivation comes from the recent work [21] on vascular prostheses called drug-eluting stents. Based on

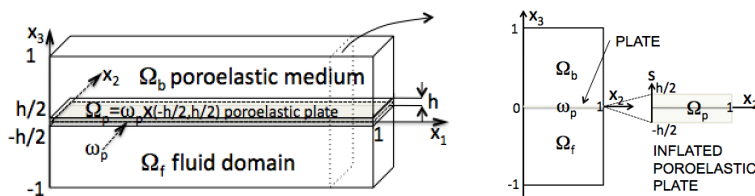


FIG. 1. Left: Three-dimensional domain Ω . Right: Two-dimensional vertical cross-section through domain Ω .

mathematical and computational results, together with experiments cited in [21], it was found that the implantation of a vascular stent within the arterial wall, induces a change in vascular tissue permeability, which is affected by the change in porosity near the end points (edges) of vascular stents. As a consequence, this can influence drug advection, reaction, and diffusion into the vascular tissue and lower the efficacy of antiinflammatory drugs in lowering restenosis (or reclosure) of coronary arteries near the edges of a stent. Thus, in the present paper we accommodate the case when *permeability is not constant, but depends on porosity*, and, in turn, on the so-called *Biot fluid content*. We note that the nonlinear permeability (dependent on fluid content) introduces *significant complications in the analysis* of the system. Such a nonlinear model was first considered—from a mathematical point—in [22], and later in [14]. The reference [22] focuses on the *compressible Biot model*, with a permeability that depends on the Biot dilation, and constructs weak solutions through a full spatio-temporal discretization in the mathematically simplified framework of homogeneous boundary conditions for both fluid pressure and solid displacement. The later reference [14] focuses on *Biot models with incompressible constituents* and constructs weak solutions following the approach of [54] for both poroelastic and poro-visco-elastic systems. Another main contribution of [14] is the treatment of nonhomogeneous, mixed boundary conditions that are physically relevant to ophthalmological applications.

The mathematical literature dealing with FPSI problems is scarce. We mention the semigroup approach based on the variational formulation of a linear *compressible* Stokes system coupled to a Biot dynamics developed in [48]. The incompressible Stokes case, considered in the present manuscript, does not seem to be covered by this analysis. Later, in [24], the problem of linear coupling (across a fixed interface) of the incompressible Navier–Stokes equations and *linear* Biot equations was considered, and the existence of *strong solutions* was proved under a small data assumption. And finally, we mention a well-posedness result for the stationary non-Newtonian fluid flow coupled with the Biot equation via fixed interface, reported in [1]. To the best of our knowledge there are no results related to the well-posedness of the FPSI problems in cases where the poroelastic model is nonlinear, and additionally, consists of multiple layers.

In the present paper we prove the *existence* of a weak solution to a fluid-structure interaction problem between the flow of an incompressible, viscous fluid and a multilayered poroelastic structure, where the Biot model in the thick poroelastic layer may be nonlinear through the dependence of permeability on the porosity. We consider two cases: the linear case in which the permeability in the Biot model may be a given function of space and time and the nonlinear, *quasi-static* case in which the permeability in the Biot model may generally depend on porosity. The proof is based on the construction of approximate solutions via Rothe’s method, introduced in [40] to study fluid-structure interaction problems between the flows of incompressible, vis-

cous fluids and *elastic* structures. The method is extended in the present paper to the poroelastic case, where the thin poroelastic plate serves as a fluid-structure interface and plays the role of a regularizing mechanism in the existence proof, similar to the results in [4, 39, 41]. The proof is based on a construction of approximate solutions by semidiscretizing the coupled problem in time and “solving” a sequence of elliptic problems for each fixed time step Δt . Using energy methods, we show that as $\Delta t \rightarrow 0$, approximate solutions converge to a weak solution of the underlying coupled problem. In the nonlinear case, a compactness argument, based on a version of the Aubin–Lions lemma, is used to show strong convergence of subsequences to a weak solution. Finally, for the linear problem we demonstrate uniqueness in a class of solutions with slightly improved regularity compared to weak solutions. For the nonlinear problem, we show a weak-strong type uniqueness result for the same class. This weak-strong uniqueness result for the FPSI with the nonlinear, quasi-static Biot model considered here is new, since even for the nonlinear Biot model alone, a full uniqueness result seems to be lacking.

We finish this introduction by mentioning that the development of numerical methods for FPSI problems has been a very active research area in the last decade (see, e.g., [2, 5, 18] and the references therein). Many problems remain open in this field, especially related to the design of partitioned schemes for FPSI problems. In particular, one of the approaches currently under investigation is the design of a partitioned scheme that would be based on the main steps in the constructive proof presented in this manuscript.

We conclude this section by noting that extensions of this work to the moving interface case, in which the fluid domain is not fixed but moving with the interface itself, require careful consideration. Such an analysis would be similar, but more complicated than those presented by the authors in [13, 40, 41], where FSI with multilayered structures and elasticity were considered, but without poroelasticity. This is one of the goals of our future research.

2. Mathematical formulation.

2.1. Spatial domain. We consider the domain $\Omega \subset \mathbb{R}^3$ with the simplest geometry describing the coupling between the flow of an incompressible, viscous fluid and a thick poroelastic medium, where the coupling occurs through a thin poroelastic plate, serving as a fluid-structure interface with mass. Namely, our domain is a rectangular prism, $\Omega = (0, 1) \times (0, 1) \times (-1, 1)$, with three distinct subregions (see Figure 1): Ω_f , which is occupied by a viscous, incompressible fluid, Ω_b , which contains a (thick) poroelastic medium modeled by the Biot’s model, and Ω_p corresponding to a thin poroelastic plate of thickness h , whose middle surface, denoted by ω_p , separates the regions Ω_f and Ω_b :

$$\begin{aligned}\Omega_f &= (0, 1)^2 \times (-1, 0), & \Omega_b &= (0, 1)^2 \times (0, 1), \\ \omega_p &= (0, 1)^2 \times \{0\}, & \Omega_p &= (0, 1)^2 \times (-h/2, h/2).\end{aligned}$$

In Cartesian coordinates (x_1, x_2, x_3) , the physical domain Ω is the union $\Omega = \Omega_f \cup \omega_p \cup \Omega_b$. The variable x_3 will be referred to as the “transverse” variable $x_3 \in [-1, 1]$, and $x_1 \in [0, 1]$ and $x_2 \in [0, 1]$ will be called the “longitudinal” and “lateral” variables, respectively.

To study filtration through the thin, poroelastic plate of thickness h , we will consider a “2.5-dimensional model,” derived and rigorously justified by Marciniak-Czochra and Mikelić in [36], obtained via asymptotic reduction from the full Biot

model. In the poroelastic plate model, the elastodynamics of the thin plate is described in terms of the x_1 and x_2 variables, as usual, namely, it is given in terms of the plate displacement of the middle surface, which is a function of only x_1 and x_2 . Filtration, however, needs to be described in terms of an additional variable $s \in [-h/2, h/2]$, since it was shown in [36] that filtration through a thin poroelastic isotropic structure is dominant in the thin/transverse direction. Therefore, we denote by ω_p the location of the middle surface of the elastic plate and by Ω_p the “inflated” mathematical domain on which the filtration velocity and pore fluid pressure will be defined. In section 2.2 we present the model, and provide more details about the approach.

The fluid contained in region Ω_f will be modeled by the time-dependent Stokes equations, with periodic boundary conditions at $x_1 = 0, x_1 = 1, x_2 = 0$, and $x_2 = 1$, and with the no-slip boundary condition at the bottom boundary $x_3 = -1$, which is considered fixed. The boundary conditions at the top fluid domain boundary, where the bulk fluid flow in Ω_f is coupled to the filtration flow in through the poroelastic membrane Ω_p , will be described in section 2.2.

Finally, Ω_b represents a thick poroelastic region relative to the thin poroelastic plate, with filtration flow and structure displacement satisfying Biot’s equations. The thick structure displacement in Ω_b , as well as the filtrate flow, will satisfy periodic boundary conditions at $x_1 = 0, x_1 = 1, x_2 = 0$, and $x_2 = 1$. At the top boundary of Ω_b , with the reference configuration described by $x_3 = 1$, we prescribe zero elastic stress and no filtration through the wall. At the bottom boundary, both the elastodynamics of the thick poroelastic medium, as well as filtration flow in Ω_b , are fully coupled to the elastodynamics and filtration flow in the thin poroelastic plate Ω_p , which is, in turn, fully coupled to the fluid flow in Ω_f . The filtration flow in Ω_b , is driven by the pressure gradient between the bottom boundary $x_3 = 0$ and the top boundary $x_3 = 1$, and by the time-dependent change in structure displacement.

In summary, the boundary of Ω consists of the periodic boundary at $x_1 = 0, x_1 = 1, x_2 = 0$, and $x_2 = 1$, a fixed bottom boundary $x_3 = -1$, and the top boundary with the reference configuration described by $x_3 = 1$. Detailed boundary conditions, and the coupling between different subdomains of Ω , will be described in the next section.

2.2. Mathematical models. In this section we describe the mathematical models, holding in each of the subdomains specified above, and specify the coupling between them. We will be using \mathbf{x} to denote points in Cartesian coordinates $\mathbf{x} = (x_1, x_2, x_3)$, the subscript b will be used to denote quantities in the Biot domain Ω_b , and subscript p will be used to denote the quantities corresponding to the poroelastic plate.

2.2.1. Biot model in Ω_b . Domain Ω_b denotes a poroelastic medium, modeled by the following Biot model, given in terms of the unknown functions $\boldsymbol{\eta} = \boldsymbol{\eta}(\mathbf{x}, t)$, describing displacement of the solid matrix from its reference configuration Ω_b , and $p_b = p_b(\mathbf{x}, t)$ denoting the pore fluid pressure:

$$(2.1) \quad \begin{cases} \rho_b \boldsymbol{\eta}_{tt} - \mu_b \Delta \boldsymbol{\eta} - (\mu_b + \lambda_b) \nabla (\nabla \cdot \boldsymbol{\eta}) + \alpha_b \nabla p_b = \mathbf{F}_b & \text{in } \Omega_b \times (0, T), \\ [c_b p_b + \alpha_b \nabla \cdot \boldsymbol{\eta}]_t - \nabla \cdot (k_b \nabla p_b) = S & \text{in } \Omega_b \times (0, T). \end{cases}$$

On the right-hand side, $\mathbf{F}_b = \mathbf{F}_b(\mathbf{x}, t)$ denotes a body force per unit volume, and $S = S(\mathbf{x}, t)$ is a net volumetric fluid production rate. The first equation describes the balance of linear momentum for the fluid-solid mixture, and the second equation

describes conservation of mass for the fluid component. The parameter coefficients in this model are the following:

	<u>Coefficients</u>	<u>Name</u>
	ρ_b	Density of poroelastic matrix;
	λ_b, μ_b	Lamé constants;
(2.2)	α_b	Biot–Willis coefficient [49];
	c_b	Constrained storage coefficient;
	k_b	Permeability of the poroelastic matrix.

In our work, we will allow the permeability k_b of the poroelastic matrix to be a nonlinear function of one variable, which we specify below in Assumption (1). We will also consider the case when the permeability k_b is a given function of \mathbf{x} and t . All other coefficients listed above will be taken constant in this analysis.

System (2.1) is obtained from the following system describing the balance of linear momentum for the fluid-solid mixture, and conservation of mass for the fluid content, denoted by ζ (see (2.9) below to recall the definition of fluid content):

$$(2.3) \quad \begin{cases} \rho_b \boldsymbol{\eta}_{tt} - \nabla \cdot \boldsymbol{\sigma}_b = \mathbf{F}_b(\mathbf{x}, t) & \text{in } \Omega_b \times (0, T), \\ \zeta_t + \nabla \cdot \mathbf{u}_b = S(\mathbf{x}, t) & \text{in } \Omega_b \times (0, T), \end{cases}$$

where \mathbf{u}_b denotes the discharge/filtration velocity associated with the pore pressure p_b and $\boldsymbol{\sigma}_b$ denotes the poroelastic stress tensor, which is given by

$$\boldsymbol{\sigma}_b = \boldsymbol{\sigma}^E - \alpha_b p_b \mathbf{I} \quad \text{in } \Omega_b \times (0, T),$$

where $\boldsymbol{\sigma}^E$ denotes a given elasticity stress tensor, and \mathbf{I} represents the identity tensor. To close the system, two constitutive laws need to be prescribed, plus Darcy's law:

1. The constitutive law $\boldsymbol{\sigma}^E = \boldsymbol{\sigma}^E(\boldsymbol{\eta})$, describing the elastic material properties: we assume the Saint Venant–Kirchhoff material:

$$(2.4) \quad \boldsymbol{\sigma}^E = 2\mu_b \mathbf{D}(\boldsymbol{\eta}) + \lambda_b \text{tr} \mathbf{D}(\boldsymbol{\eta}) \mathbf{I} = 2\mu_b \mathbf{D}(\boldsymbol{\eta}) + \lambda_b \nabla \cdot \boldsymbol{\eta} \mathbf{I},$$

where λ_b, μ_b denote the Lamé constants, and $\mathbf{D}(\boldsymbol{\eta}) = \frac{1}{2}(\nabla \boldsymbol{\eta} + (\nabla \boldsymbol{\eta})^T)$ represents the symmetrized gradient.

2. The constitutive law $\zeta = \zeta(p_b, \boldsymbol{\eta})$, defining the fluid content in terms of the fluid pore pressure, and the “compressibility of the solid matrix,” i.e., the change in the pore volume,

$$(2.5) \quad \zeta = c_b p_b + \alpha_b \nabla \cdot \boldsymbol{\eta},$$

where $c_b \geq 0$ and $\alpha_b > 0$ were introduced in (2.2). Note that the case $c_b = 0$ is permitted below, and this corresponds to *incompressible constituents* in the poroelastic material.

3. Darcy's law:

$$(2.6) \quad \mathbf{u}_b = -\mathbf{K} \nabla p_b \quad \text{with} \quad \mathbf{K} = k_b \mathbf{I},$$

where \mathbf{K} is the permeability tensor.

By using these constitutive laws in system (2.3), one recovers (2.1). Notice that system (2.1) is obtained under the assumption of small deformations.

Assumption 1. When considering the case of nonlinear permeability, we assume that the permeability tensor \mathbf{K} is a *nonlinear function of porosity* ϕ :

$$(2.7) \quad \mathbf{K} = k_b \mathbf{I} \text{ with } k_b = k_{\text{ref}} f_k(\phi),$$

where k_{ref} is a reference value for the permeability of the mixture given in terms of the volumetric fraction ϕ of the fluid component, called *porosity*. The particular form of the relationship between the permeability k_b and the porosity ϕ is represented by the function $f_k(\phi)$, and it depends on the geometrical architecture of the pores inside the matrix and the physical properties of the fluid [23, 33].

For completeness, we recall the definitions of *porosity* ϕ and *fluid content* ζ . Porosity ϕ is defined as the volumetric fraction

$$(2.8) \quad \phi = \frac{V_f(\mathbf{x}, t)}{V(\mathbf{x}, t)}$$

of the volume $V_f(\mathbf{x}, t)$ occupied by the fluid within the poroelastic medium and the representative elementary volume of the poroelastic medium $V(\mathbf{x}, t)$, centered at $\mathbf{x} \in \Omega_b$ at time t .

Similarly, if we denote by $V_s(\mathbf{x}, t)$ the volume occupied by the solid, then under the assumption of fully saturated mixture, the volumetric fraction $V_s(\mathbf{x}, t)/V(\mathbf{x}, t) = 1 - \phi(\mathbf{x}, t)$.

Fluid content ζ is the increment in the volumetric fraction of the fluid component ϕ with respect to its baseline value ϕ_0 :

$$(2.9) \quad \zeta(\mathbf{x}, t) = \phi(\mathbf{x}, t) - \phi_0(\mathbf{x}).$$

Notice that the constitutive law for the fluid content (2.5) implies that porosity is given by

$$\phi = \phi(p_b, \boldsymbol{\eta}) = \phi_0 + c_b p_b + \alpha_b \nabla \cdot \boldsymbol{\eta}.$$

Thus, under the nonlinearity assumption, specified in Assumption 1, we have

$$(2.10) \quad k_b = k_b(\phi) = k_b(\phi(p_b, \nabla \cdot \boldsymbol{\eta})) = k_b(c_b p_b + \alpha_b \nabla \cdot \boldsymbol{\eta}).$$

For analysis purposes, we will be assuming the following properties of the permeability function k_b .

Assumption 2. We assume that the permeability function $k_b : \mathbb{R} \rightarrow \mathbb{R}$ is continuous and that there exist constants $k_{\min} > 0$ and $k_{\max} > 0$ s.t.

$$0 < k_{\min} \leq k_b(\zeta) \leq k_{\max} \quad \forall \zeta \in \mathbb{R}.$$

In consideration of the *linear* dynamics below, we will consider $k_b = k_b(\mathbf{x}, t)$ to be a given space and time dependent function. In the nonlinear considerations, we will denote by $k_b(\Psi(x))$ the Nemytskii operator associated with k_b . In that situation, our assumptions on the function k_b , and the theory of superposition operators [44, 52], will yield that the operator k_b is bounded and continuous from $L^2(\Omega \times (0, T))$ into $L^2(\Omega \times (0, T))$. In our consideration of uniqueness for the nonlinear problem below, we will consider the hypotheses that k_b is a globally Lipschitz function on \mathbb{R} .

Remark 2.1. As in [14], we could also consider a poroviscoelastic material, for which the stress tensor $\boldsymbol{\sigma}_b$ would include a viscoelastic component, for example,

$$(2.11) \quad \boldsymbol{\sigma}_b = \boldsymbol{\sigma}^E + \boldsymbol{\sigma}^V - \alpha_b p_b \mathbf{I}, \quad \boldsymbol{\sigma}^V = 2\mu_V \mathbf{D}(\boldsymbol{\eta}_t) + \lambda_V \text{tr} \mathbf{D}(\boldsymbol{\eta}_t) \mathbf{I},$$

where λ_V and μ_V are independent Lamé parameters for viscoelasticity. All the results from this manuscript would hold for the viscoporoelastic case as well.

2.2.2. Poroelastic plate model in Ω_p . Domain Ω_p denotes a thin, poroelastic plate, separating the fluid flow region Ω_f , from the thick, poroelastic structure in Ω_b . A plate is a thin, three-dimensional region, bounded by two surfaces of small curvature, whose distance defines the thickness of the plate. In our case, the plate will be assumed to be flat and of uniform thickness h , with the two surfaces located at $h/2$ distance on either side of the *middle surface* of the plate, denoted by ω_p . The reference configuration of the middle surface ω_p is $x_3 = 0$.

We will be assuming that the elastic plate is porous, isotropic, and saturated by a viscous fluid. To capture the elastic deformation of the poroelastic skeleton, as well as fluid flow through the skeleton pores, we will be using a model which is a dynamic version of the quasi-static Biot poroelastic plate model, studied by Biot in [11], and rigorously justified by Marciniak-Czochra and Mikelić in [36]. This model was obtained under the following hypotheses.

Assumption 3. Poroelastic plate hypotheses:

1. The Kirchhoff hypothesis: Every straight line in the plate that was originally perpendicular to the plate's middle surface remains straight and perpendicular to the deflected middle surface after deformation.
2. The fluid velocity derivatives in the longitudinal and lateral directions are small compared to the transverse one.

Therefore, the dominant flow is in the transverse direction.

The resulting equations are given in terms of displacement $\mathbf{w} = \mathbf{w}(x_1, x_2)$ of the plate's middle surface from its reference configuration ω_p , where $(x_1, x_2) \in \omega_p$, and the fluid pore pressure p_p , where p_p is a function of three variables: two corresponding to the coordinates along the middle surface ω_p , and the third one, denoted by $s \in (-h/2, h/2)$, corresponding to the *local transverse* coordinate, so that $p_p = p_p(x_1, x_2, s)$, where $(x_1, x_2, s) \in \Omega_p$.

According to [36], for small deflections and s -driven pressure gradients, the in-plane and transverse plate dynamics fully decouple. Since in our problem the stress in the transverse direction is larger than the stress in the longitudinal and lateral directions, we consider only the *transverse plate displacement*, which we denote by $w(x_1, x_2, t)$, where $(x_1, x_2) \in \omega_p$. For each s slice in $(-h/2, h/2)$, the w dynamics is constant. However, the fluid pore pressure $p_p(x_1, x_2, s)$ can vary for $s \in (-h/2, h/2)$. The resulting reduced Biot model for a poroelastic plate is then given by two equations, one describing poroelastodynamics, which will be defined in ω_p , and one describing conservation of mass of the fluid phase, given in terms of the evolution of p_p , defined in Ω_p [11, 26, 31, 36]:

$$(2.12) \quad \begin{cases} \rho_p w_{tt} + D \Delta_{\omega_p}^2 w + \gamma w + \alpha_p \Delta_{\omega_p} \int_{-h/2}^{h/2} s p_p \, ds = F_p(x_1, x_2, t) & \text{in } \omega_p \times (0, T), \\ \partial_t [c_p p_p - \alpha_p s \Delta_{\omega_p} w] - \partial_s (k_p \partial_s p_p) = 0 & \text{in } \Omega_p \times (0, T). \end{cases}$$

All Laplacians above refer to the in-plane Laplacian, i.e., $\Delta_{\omega_p} = \partial_{x_1}^2 + \partial_{x_2}^2$. The constant $D > 0$ is the elastic stiffness coefficient for the plate, and $\gamma > 0$ is an [elastic] coefficient that we added for technical reasons to provide coercivity, since coercivity is not automatically satisfied in the periodic framework. The constants ρ_p , α_p , c_p , and k_p are the same as those in (2.2), taken for the poroelastic plate. One distinction for the poroelastic plate is that our results below will require $c_p > 0$. The source term F_p corresponds to the loading of the poroelastic plate, which will come from the jump in the normal components of the normal stress (traction) between the fluid

on one side and the thick Biot poroelastic structure on the other: $F_p(x_1, x_2, t) = \sigma_b \mathbf{e}_3 \cdot \mathbf{e}_3|_{\omega_p} - \sigma_f \mathbf{e}_3 \cdot \mathbf{e}_3|_{\omega_p}$. This will be specified below in the coupling conditions (2.20). As before, Darcy's law, relating the filtration velocity to the pressure gradient, holds here:

$$(2.13) \quad u_p = -k_p \partial_s p_p \quad \text{in } \Omega_p \times (0, T)$$

where u_p denotes the transverse (dominant) component of filtration velocity, relative to the motion of the poroelastic matrix.

2.2.3. Time-dependent Stokes model in Ω_f . In the lower half space, denoted by Ω_f , we consider the flow of a viscous, incompressible fluid modeled by the time-dependent Stokes equations:

$$(2.14) \quad \left. \begin{aligned} \rho_f \frac{\partial \mathbf{u}}{\partial t} &= \nabla \cdot \boldsymbol{\sigma}_f + \mathbf{f} \\ \nabla \cdot \mathbf{u} &= 0 \end{aligned} \right\} \text{ in } \Omega_f \times (0, T),$$

where \mathbf{u} is the fluid velocity, $\boldsymbol{\sigma}_f = 2\mu_f \mathbf{D}(\mathbf{u}) - p_f \mathbf{I}$ is the Cauchy stress tensor, p_f is the fluid pressure, ρ_f is the fluid density, and μ_f is the fluid viscosity with $\mathbf{D}(\mathbf{u})$ denoting the fluid strain-rate tensor (symmetrized gradient of velocity).

The fluid interacts with the multilayered poroelastic structure by exerting stress onto the poroelastic structure that causes deformation of the poroelastic skeleton, while at the same time generating the pressure difference, or more generally, the normal stress difference across the poroelastic plate, causing filtration flow through the poroelastic plate and on to the Biot poroelastic medium. The poroelastic plate serves as a fluid-structure interface with mass, which will provide a regularizing mechanism in the analysis of this fluid-structure interaction problem.

In summary, the following are the three models holding in the three different subdomains of Ω :

$$(2.15) \quad \left\{ \begin{aligned} \rho_b \boldsymbol{\eta}_{tt} - \mu_b \Delta \boldsymbol{\eta} - (\mu_b + \lambda_b) \nabla (\nabla \cdot \boldsymbol{\eta}) + \alpha_b \nabla p_b &= \mathbf{F}_b, & (x_1, x_2, x_3) \in \Omega_b, \\ [c_b p_b + \alpha_b \nabla \cdot \boldsymbol{\eta}]_t - \nabla \cdot (k_b \nabla p_b) &= S, & (x_1, x_2, x_3) \in \Omega_b, \end{aligned} \right.$$

$$(2.16) \quad \left\{ \begin{aligned} \rho_p w_{tt} + D \Delta_{\omega_p}^2 w + \gamma w + \alpha_p \Delta_{\omega_p} \int_{-h/2}^{h/2} s p_p \, ds &= F_p, & (x_1, x_2) \in \omega_p, \\ [c_p p_p - \alpha_p s \Delta_{\omega_p} w]_t - \partial_s (k_p \partial_s p_p) &= 0, & (x_1, x_2, s) \in \Omega_p, \end{aligned} \right.$$

$$(2.17) \quad \left\{ \begin{aligned} \rho_f \mathbf{u}_t - \mu_f \Delta \mathbf{u} + \nabla p_f &= \mathbf{f}, & (x_1, x_2, x_3) \in \Omega_f, \\ \nabla \cdot \mathbf{u} &= 0, & (x_1, x_2, x_3) \in \Omega_f. \end{aligned} \right.$$

Remark 2.2. The notation for k_b here (and below) in the problem description is general, so that it can accommodate the linear and nonlinear cases simultaneously.

2.2.4. Coupling conditions. The coupling between the fluid and multilayered poroelastic structure is assumed at the poroelastic plate, which serves as a fluid-structure interface with mass. The coupling conditions describe the relationship between the kinematic quantities, such as velocities (and consequently displacements),

and the balance of forces. One set of coupling conditions will be prescribed across the middle surface of the plate ω_p , and the other set of coupling conditions will be prescribed across the top and bottom surfaces on the plate, which we denoted by ω_p^+ and ω_p^- . The top and bottom surfaces are defined in terms of the “inflation variable” s as follows:

$$(2.18) \quad \begin{aligned} \omega_p^+ &= (0, 1)^2 \times \{h/2\} \\ &= \{(x_1, x_2, s) | (x_1, x_2) \in \mathbb{R}^2, s = 1/2\}, \quad \text{and} \quad \omega_p^- = (0, 1)^2 \times \{-h/2\}. \end{aligned}$$

The coupling conditions along the middle surface of the plate ω_p are in line with the Kirchhoff hypothesis for plates (see Assumption 3) in the sense that those conditions are given in terms of displacement w of the middle surface of the plate, which is only a function of x_1 and x_2 , and therefore the coupling is along ω_p . Across ω_p , we prescribe the behavior of the *structure* velocity $\partial_t w$ (the kinematic coupling condition) and the forces that drive the motion of the middle surface of the plate (the dynamic coupling condition). Across ω_p^+ and ω_p^- we prescribe the continuity of vertical components of *fluid* velocity (the kinematic coupling condition) and the balance of normal components of normal stress (the dynamic coupling condition).

One novelty of the proposed model is the coupling in the pressure. See Remark 2.3. As we shall see below, the coupling of the plate filtration pressure at the top interface ω_p^+ and at the bottom interface ω_p^- with the surrounding fluid pressure will give rise to a pressure jump between the top and bottom interface, which is what drives the filtration flow through the plate.

1. *Coupling across the plate's middle surface ω_p .* We have two sets of coupling conditions, the kinematic and dynamic. For the kinematic coupling condition, we assume continuity between the plate displacement and the Biot displacement evaluated at the interface ω_p , while on the fluid side we assume the Beavers–Joseph–Saffman coupling condition, stating that the tangential components of the fluid velocity evaluated at ω_p are proportional to the corresponding tangential components of the fluid normal stress evaluated at ω_p . The constant of proportionality, denoted by β , denotes the *slip length*. For the dynamic coupling (see (2.20) below), we state that the elastodynamics of the poroelastic plate is driven by the jump in the normal components of normal stress between the fluid and Biot poroelastic medium, where the jump is evaluated at the two-dimensional fluid-structure interface ω_p . Here F_p is the forcing from the plate equation (2.16):

$$(2.19) \quad \begin{cases} \langle 0, 0, w \rangle &= \boldsymbol{\eta}|_{\omega_p}, \\ \beta \mathbf{u}|_{\omega_p} \cdot \mathbf{e}_i &= -[\boldsymbol{\sigma}_f|_{\omega_p} \mathbf{e}_3] \cdot \mathbf{e}_i, \quad i = 1, 2, \end{cases}$$

$$(2.20) \quad F_p = \boldsymbol{\sigma}_b \mathbf{e}_3 \cdot \mathbf{e}_3|_{\omega_p} - \boldsymbol{\sigma}_f \mathbf{e}_3 \cdot \mathbf{e}_3|_{\omega_p},$$

We remark here that the first condition in (2.19) is the continuity of vertical components of structure velocities (assuming equal structural displacements initially), and the second condition in (2.19) in fact reads

$$(\beta \mathbf{u}|_{\omega_p} - \partial_t \mathbf{w}) \cdot \mathbf{e}_i = -[\boldsymbol{\sigma}_f|_{\omega_p} \mathbf{e}_3] \cdot \mathbf{e}_i, \quad i = 1, 2,$$

where the left-hand side is the tangential velocity slip. However, since the full Lagrangian plate displacement $\mathbf{w} = \langle 0, 0, w \rangle$, the tangential components ($i = 1, 2$) of $\partial_t \mathbf{w}$ are both equal to zero.

2. *Coupling across the Biot-plate interface (ω_p^+).* Here we specify the coupling that involves the quantities that are defined on the inflated plate domain Ω_p , such as

filtration velocity and pore pressure, and couple them to the corresponding quantities in the Biot model. For this purpose, we evaluate the plate quantities at the inflated surface ω_p^+ , defined in (2.18), and the Biot quantities at the interface portion of the boundary of the Biot domain, namely, on ω_p . In particular, we assume the continuity of filtration velocities, which are defined relative to the motion of the poroelastic matrix $\mathbf{u}_b \cdot \mathbf{e}_3 = u_p$, and continuity of pore pressures. Using Darcy's laws (2.6) and (2.13), the two coupling conditions read

$$(2.21) \quad k_p \partial_s p_p|_{\omega_p^+} = k_b \partial_{x_3} p_b|_{\omega_p},$$

$$(2.22) \quad p_p|_{\omega_p^+} = p_b|_{\omega_p}.$$

We remark here that condition (2.21) describes continuity of vertical components of filtration velocities (relative to the elastic structure motion), after accounting for Darcy's law.

3. *Coupling across the Stokes-plate interface (ω_p^-).* Similarly to the coupling presented above, here we specify the coupling of the quantities defined on the inflated plate domain Ω_p , namely, the plate filtration velocity and pressure, with the Stokes flow. Again, we evaluate the plate quantities at the inflated surface ω_p^- adjacent to the fluid domain and the Stokes quantities at the interface boundary of the fluid domain, and the Stokes quantities at the interface boundary of the fluid domain, namely, on ω_p . In particular, we assume continuity of filtration velocities relative to the motion of the poroelastic matrix, $w_t - (\mathbf{u} \cdot \mathbf{e}_3)|_{\omega_p} = u_p$, and continuity of the normal component of the normal fluid stress. Using Darcy's law (2.13), the two coupling conditions read:

$$(2.23) \quad w_t - (\mathbf{u} \cdot \mathbf{e}_3)|_{\omega_p} = k_p \partial_s p_p|_{\omega_p^-},$$

$$(2.24) \quad -\boldsymbol{\sigma}_f \mathbf{e}_3 \cdot \mathbf{e}_3|_{\omega_p} = p_p|_{\omega_p^-}.$$

We remark that condition (2.23) describes continuity of vertical components of velocities (relative to the structure motion), where the fluid velocity on the left-hand side is corrected by the velocity of the structure w_t .

Remark 2.3. By combining the coupling conditions for the fluid pressure given in (2.22) and (2.24), we see that across the FPSI interface, the pressure (the normal component of normal stress, in fact) jumps from $-\boldsymbol{\sigma}_f \mathbf{e}_3 \cdot \mathbf{e}_3|_{\omega_p}$ on the fluid side to $p_b|_{\omega_p}$ on the Biot side. In between, a pressure gradient-driven vertical/transverse flow through the poroelastic plate takes place from $p_p|_{\omega_p^-}$ to $p_p|_{\omega_p^+}$. Thus, the jump in the pressure at the interface ω_p (namely, the jump in the normal components of normal stress), given by $[p_b - \boldsymbol{\sigma}_f \mathbf{e}_3 \cdot \mathbf{e}_3]$ on ω_p , drives the filtration flow through the interface, i.e., through the poroelastic plate.

2.2.5. Boundary and initial conditions. Boundary conditions on $\partial\Omega$.

We take periodic boundary conditions for all quantities of interest in the longitudinal and lateral directions and identify $x_i = 0$ with $x_i = 1$ for $i = 1, 2$.

For $x_3 = -1$, we consider the standard *no-slip* boundary conditions for the Stokes fluid, i.e., $\mathbf{u} \equiv \mathbf{0}|_{x_3=-1}$. For $x_3 = 1$, we take Neumann-type (homogeneous) boundary conditions for the Biot system.

We summarize the boundary conditions in the following table:

	Region	Functions	Boundary condition
(2.25)	$x_i = 0, x_i = 1, i = 1, 2$	$\boldsymbol{\eta}, w, p_b, \mathbf{u}$	Periodic
(2.26)	$x_3 = -1$	\mathbf{u}	$\mathbf{u} _{x_3=-1} = \mathbf{0}$
(2.27)	$x_3 = 1$	$\boldsymbol{\eta}, p_b$	$\boldsymbol{\sigma}(\boldsymbol{\eta}, p_b)\mathbf{e}_3 = \mathbf{0}, \partial_{x_3}p_b = 0$

Remark 2.4. Note that we do not prescribe boundary conditions for p_p on the lateral boundaries, owing to the structure of the pressure equation for the poro-plate. This is to say, there is no differential operator acting on p_p in the tangential directions, and thus no boundary conditions to be prescribed. We will see this also in the functions spaces prescribed below in section 3.2.

Initial conditions at $t = 0$:

$$(2.28) \quad \text{Fluid: } \mathbf{u}(., 0) = \mathbf{u}^0,$$

$$(2.29) \quad \text{Poroelastic plate: } w(., 0) = w^0, \partial_t w(., 0) = \dot{w}^0, p_p(., 0) = p_p^0,$$

$$(2.30) \quad \text{Biot equations: } \boldsymbol{\eta}(., 0) = \boldsymbol{\eta}^0, \partial_t \boldsymbol{\eta}(., 0) = \dot{\boldsymbol{\eta}}^0, p_b(., 0) = p_b^0.$$

Here, we used \dot{w}^0 and $\dot{\boldsymbol{\eta}}^0$ to denote the initial data for the time derivative of w and $\boldsymbol{\eta}$, respectively.

2.3. Quasi-static problem. The *quasi-static* version of problem (2.15)–(2.30) refers to the problem in which the inertial effects in the Biot model (2.1) are neglected:

Assumption 4. The quasi-static model refers to setting $\rho_b = 0$ in (2.15) and allowing $\rho_p \geq 0$ in (2.16).

This quasi-static assumption arises naturally in the classical Biot model of consolidation for a linearly elastic and porous solid which is saturated by a slightly compressible viscous fluid. See, e.g., [49]. The quasi-static assumption requires modifying the initial conditions, but leaves the coupling conditions the same. As we shall see in section 6, we can extend our linear existence result to the nonlinear case *when* Assumption 4 is taken. On the other hand, it has been noted by many authors that the elliptic-parabolic nature of the quasi-static Biot problem presents its own challenges [16, 49].

The new *initial conditions*, owing to loss of acceleration terms, are given by the following:

- If $\rho_b = 0$, initial conditions (2.30) are replaced with initial condition for the fluid content:

$$(2.31) \quad \zeta_b(., 0) = (c_b p_b + \alpha_b \nabla \cdot \boldsymbol{\eta})(., 0) = \zeta_b^0.$$

- If $\rho_p = 0$, initial conditions (2.29) are replaced with initial condition for the poroelastic plate fluid content:

$$(2.32) \quad \zeta_p(., 0) = (c_p p_p - \alpha_p s \Delta_{\omega_p} w)(., 0) = \zeta_p^0.$$

In the analysis of such quasi-static Biot models (see [14, 16, 22, 43, 49, 54]), the structure of the initial condition is a nontrivial issue. In this treatment, we only consider ζ_b^0 for which there exist $\boldsymbol{\eta}^0 = \boldsymbol{\eta}(0)$ and $p_b^0 = p_b(0)$ s.t. $c_b p_b^0 + \alpha_b \nabla \cdot \boldsymbol{\eta}^0 = \zeta_b^0$. Such a hypothesis is common [14, 22, 54].

Remark 2.5. For a very weak notion of a solution in the linear case, the work in [47, 49] only requires initial conditions as specified above, which is to say, for the respective fluid contents alone. However, in nearly every other construction, additional regularity of the initial condition is required. This is a by-product of using a priori estimates to construct solutions. See [54, Remark 2] and [49, p. 327], where this is explicitly discussed.

Details of the existence result are given in section 6.

3. Energy, function spaces, and weak formulation. In this section we derive a formal energy estimate, present functions spaces for the solution, and define a weak solution. For this purpose, we recall the principal solutions variables in each subregion:

- (\mathbf{u}, p_f) —Stokes fluid velocity and pressure defined on Ω_f ;
- (w, w_t, p_p) —transverse displacement and velocity of the poroelastic plate and poroelastic plate pressure, defined on ω_p and Ω_p , respectively;
- $(\boldsymbol{\eta}, \boldsymbol{\eta}_t, p_b)$ —poroelastic displacement, velocity, and pressure defined on Ω_b (thick Biot region). The quantity $\mathbf{u}_b = -\mathbf{K}\nabla p_b = -k_b(c_b p_b + \alpha_b \nabla \cdot \boldsymbol{\eta})\nabla p_b$ is the discharge velocity in thick poroelastic material.

3.1. A formal energy inequality. By testing equations (2.15)–(2.17) by the solution variables, specified above, and by using coupling conditions (2.19)–(2.24), and periodic boundary conditions, we obtain the following formal energy identity:

$$\begin{aligned}
 (3.1) \quad & \frac{1}{2} \frac{d}{dt} \left(\rho_f \|\mathbf{u}\|_{L^2(\Omega_f)}^2 + \rho_p \|w_t\|_{L^2(\omega_p)}^2 + \rho_b \|\partial_t \boldsymbol{\eta}\|_{L^2(\Omega_b)}^2 \right) \\
 & + \frac{1}{2} \frac{d}{dt} \left(c_p \|p_p\|_{L^2(\Omega_p)}^2 + \|\boldsymbol{\eta}\|_E^2 + c_b \|p_b\|_{L^2(\Omega_b)}^2 + D \|\Delta w\|_{L^2(\omega_p)}^2 + \gamma \|w\|_{L^2(\omega_p)}^2 \right) \\
 & + 2\mu_f \|D(\mathbf{u})\|_{L^2(\Omega_f)}^2 + \beta \|\mathbf{u} \cdot \boldsymbol{\tau}\|_{L^2(\omega_p)}^2 + \|k_p^{1/2} \partial_s p_p\|_{L^2(\Omega_p)}^2 + \|k_b^{1/2} \nabla p_b\|_{L^2(\Omega_b)}^2 \\
 & \leq C_{data},
 \end{aligned}$$

where

$$\|\boldsymbol{\eta}\|_E^2 = \int_{\Omega_b} [\boldsymbol{\sigma}^E : \nabla \boldsymbol{\eta}] d\mathbf{x} = 2\mu_E (D(\boldsymbol{\eta}), D(\boldsymbol{\eta}))_{L^2(\Omega_b)} + \lambda_E (\nabla \cdot \boldsymbol{\eta}, \nabla \cdot \boldsymbol{\eta})_{L^2(\Omega_b)},$$

and

$$\|\mathbf{u} \cdot \mathbf{t}\|_{L^2(\omega_p)}^2 = \sum_{i=1,2} \|\mathbf{u} \cdot \mathbf{t}_i\|^2,$$

where \mathbf{t}_i are the tangent vectors, given by $\mathbf{e}_1, \mathbf{e}_2$ on ω_p in this case. Note that the formal energy identity for the quasi-static dynamics can be obtained by letting $\rho_b = 0$, and this is valid for $\rho_p = c_b = 0$ as well. Our results will include all these cases. See section 3.3 and Remark 3.5.

Remark 3.1. We shall see later that this energy inequality will hold for constructed solutions, but need not hold in the general case for weak solutions, even in the case of linear dynamics.

3.2. Function spaces for weak solutions. For any function space X , let us introduce the notation that $X_\#$ is the space of all functions from X that are 1-periodic

in directions x_1 and x_2 :

$$X_{\#} := \{f \in X : f|_{x_1=0} = f|_{x_1=1}, f|_{x_2=0} = f|_{x_2=1}\}.$$

Stokes equation:

$$\begin{aligned} H &= \{\mathbf{u} \in \mathbf{L}^2(\Omega_f) : \nabla \cdot \mathbf{u} = 0, (\mathbf{u} \cdot \mathbf{e}_3)|_{x_3=-1} = 0\}, \\ V &= \{\mathbf{u} \in \mathbf{H}^1(\Omega_f) : \nabla \cdot \mathbf{u} = 0, \mathbf{u}|_{x_3=-1} = 0\}, \\ \mathcal{V}_f &= L^\infty(0, T; H) \cap L^2(0, T; V_{\#}). \end{aligned}$$

Poroeleastic plate:

$$\begin{aligned} H^{0,0,1} &= \{p \in L^2(\Omega_p) : \partial_s p \in L^2(\Omega_p)\} \\ \mathcal{V}_p &= \{w \in L^\infty(0, T; H_{\#}^2(\omega_p)) : \rho_p w \in W^{1,\infty}(0, T; L^2(\omega_p))\}, \\ \mathcal{Q}_p &= \{p \in L^2(0, T; H^{0,0,1}) : c_p p \in L^\infty(0, T; L^2(\Omega_p))\}. \end{aligned}$$

Biot equations:

$$\begin{aligned} \mathcal{V}_b &= \{\boldsymbol{\eta} \in L^\infty(0, T; \mathbf{H}_{\#}^1(\Omega_b)) : \rho_b \boldsymbol{\eta} \in W^{1,\infty}(0, T; \mathbf{L}^2(\Omega_b))\}, \\ \mathcal{Q}_b &= \{p \in L^2(0, T; H_{\#}^1(\Omega_b)) : c_b p \in L^\infty(0, T; L^2(\Omega_b))\}. \end{aligned}$$

Weak solution space:

$$\mathcal{V}_{\text{sol}} = \{(\mathbf{u}, w, p_p, \boldsymbol{\eta}, p_b) \in \mathcal{V}_f \times \mathcal{V}_p \times \mathcal{Q}_p \times \mathcal{V}_b \times \mathcal{Q}_b : p_p|_{s=h/2} = p_b|_{x_3=0}, \boldsymbol{\eta}|_{x_3=0} = w\mathbf{e}_3\}.$$

Remark 3.2. We included the “inertial” and “compressibility” constants in the definition of the solution spaces in order to unify the exposition and, at the same time, point to the different regularities of solutions for the different scenarios.

In conjunction with \mathcal{V}_{sol} we define the *test space* as follows:

$$\begin{aligned} (3.2) \quad \mathcal{V}_{\text{test}} &= \{(\mathbf{v}, z, q_p, \boldsymbol{\psi}, q_b) \in C_c^1([0, T]; V_{\#} \times H_{\#}^2(\omega_p) \times H^{0,0,1} \times \mathbf{H}_{\#}^1(\Omega_b) \times H_{\#}^1(\Omega_b)) \\ &\quad : q_p|_{s=h/2} = q_b|_{x_3=0}, \boldsymbol{\psi}|_{x_3=0} = z\mathbf{e}_3\}, \end{aligned}$$

where we use the standard notation C_c^1 for continuously differentiable functions with compact support.

3.3. General weak formulation. We aim to construct a function $(\mathbf{u}, w, p_p, \boldsymbol{\eta}, p_b) \in \mathcal{V}_{\text{sol}}$, called a *weak solution*, such that for every smooth test function $(\mathbf{v}, z, q_p, \boldsymbol{\psi}, q_b) \in \mathcal{V}_{\text{test}}$, the *weak formulation* specified below in Definition 1 holds. To formulate the weak formulation we introduce the following notation:

- $((\cdot, \cdot))_{\mathcal{O}}$ denotes an inner-product on $L^2(0, T; L^2(\mathcal{O}))$ for a domain \mathcal{O} ;
- $\langle \cdot, \cdot \rangle$ denotes a particular “duality” pairing whose precise interpretation will be specified below.

To obtain the weak formulation for the coupled system, we proceed by formally multiplying the equations in (2.15)–(2.17) by test functions and integrating by parts as described below.

We begin by using the test function $\psi \in C_c^1([0, T]; \mathbf{H}_\#^1(\Omega_b))$, with $\psi|_{x_3=0} = z\mathbf{e}_3$ for the balance of linear momentum equation in the Biot model (2.15), to obtain

$$(3.3) \quad -\rho_b((\boldsymbol{\eta}_t, \boldsymbol{\psi}_t))_{\Omega_b} + ((\boldsymbol{\sigma}_b(\boldsymbol{\eta}, p_b), \nabla \boldsymbol{\psi}))_{\Omega_b} - \int_0^T \int_{\partial\Omega_b} \boldsymbol{\sigma}_b(\boldsymbol{\eta}, p_b) \mathbf{n} \cdot \boldsymbol{\psi} = \rho_b(\boldsymbol{\eta}_t, \boldsymbol{\psi})|_{t=0} + ((\mathbf{F}_b, \boldsymbol{\psi}))_{\Omega_b}.$$

For the balance of mass equation, we use the test function $q_b \in C_c^1([0, T]; H_\#^1(\Omega_b))$ and obtain

$$(3.4) \quad -((c_b p_b + \alpha_b \nabla \cdot \boldsymbol{\eta}, \partial_t q_b))_{\Omega_b} + ((k_b \nabla p_b, \nabla q_b))_{\Omega_b} - \int_0^T \int_{\partial\Omega_b} k_b \nabla p_b \cdot \mathbf{n} q_b = (c_b p_b + \alpha_b \nabla \cdot \boldsymbol{\eta}, q_b)|_{t=0} + ((S, q_b))_{\Omega_b}.$$

For the equation describing the poroelastic plate dynamics (2.16), we use test function $z \in C_c^1([0, T]; H_\#^2(\omega_p))$ to obtain

$$(3.5) \quad -\rho_p((w_t, \partial_t z))_{\omega_p} + D((\Delta w, \Delta z))_{\omega_p} + \alpha_p \left(\left(\int_{-h/2}^{h/2} (s p_p) ds, \Delta z \right) \right)_{\omega_p} + \gamma((w, z))_{\omega_p} = \rho_p(w_t, z)|_{t=0} + \int_0^T \int_{\omega_p} F_p z.$$

In the conservation of mass of the fluid phase for the poroelastic plate we use the test function $q_p \in C_c^1([0, T]; H_\#^{0,0,1})$ to obtain

$$(3.6) \quad -((c_p p_p - \alpha_p s \Delta w, \partial_t q_p))_{\Omega_p} + ((k_p \partial_s p_p, \partial_s q_p))_{\Omega_p} - \int_0^T \int_{\partial\Omega_p} k_p \partial_s p_p n_3 q_p = (c_p p_p - \alpha_p s \Delta w, q_p)_{\Omega_p}|_{t=0}.$$

Finally, we use test function $\mathbf{v} \in C_c^1([0, T]; V_\#)$ in the Stokes equation (2.17), which provides

$$(3.7) \quad -\rho_f((\mathbf{u}, \mathbf{v}_t))_{\Omega_f} + \mu_f((\mathbf{D}(\mathbf{u}), \mathbf{D}(\mathbf{v})))_{\Omega_f} + \int_0^T \int_{\partial\Omega_f} \boldsymbol{\sigma}_f \mathbf{n} \cdot \mathbf{v} = \rho_f(\mathbf{u}, \mathbf{v})|_{t=0} + ((\mathbf{f}, \mathbf{v}))_{\Omega_f}.$$

Note that when we combine (3.3)–(3.7), the collection of boundary terms is represented by

$$(3.8) \quad I_{\text{bdry}} = - \int_0^T \int_{\partial\Omega_b} \boldsymbol{\sigma}_b(\boldsymbol{\eta}, p_b) \mathbf{n} \cdot \boldsymbol{\psi} - \int_0^T \int_{\omega_p} \boldsymbol{\sigma}_b \mathbf{e}_3 \cdot \mathbf{e}_3|_{\omega_p} z - \int_0^T \int_{\partial\Omega_b} k_b \nabla p_b \cdot \mathbf{n} q_b - \int_0^T \int_{\partial\Omega_p} k_p \partial_s p_p n_3 q_p + \int_0^T \int_{\omega_p} \boldsymbol{\sigma}_f \mathbf{e}_3 \cdot \mathbf{e}_3|_{\omega_p} z + \int_0^T \int_{\partial\Omega_f} \boldsymbol{\sigma}_f \mathbf{n} \cdot \mathbf{v}.$$

After using the boundary condition $\boldsymbol{\sigma}(\boldsymbol{\eta}, p_b)\mathbf{e}_3 = \mathbf{0}$ and the fact that $\boldsymbol{\psi}|_{x_3=0} = z\mathbf{e}_3$, the first term in (3.8) becomes

$$(3.9) \quad - \int_0^T \int_{\partial\Omega_b} \boldsymbol{\sigma}_b(\boldsymbol{\eta}, p_b)\mathbf{n} \cdot \boldsymbol{\psi} = - \int_{x_3=1} \boldsymbol{\sigma}_b\mathbf{e}_3 \cdot \boldsymbol{\psi} + \int_{\omega_p} \boldsymbol{\sigma}_b\mathbf{e}_3 \cdot \boldsymbol{\psi} = \int_0^T \int_{\omega_p} \boldsymbol{\sigma}_b\mathbf{e}_3 \cdot \mathbf{e}_3|_{\omega_p} z,$$

and therefore the first two terms cancel each other. The next two terms in (3.8) can be rewritten as follows:

$$(3.10) \quad - \int_0^T \int_{\partial\Omega_b} k_b \nabla p_b \cdot \mathbf{n} q_b - \int_0^T \int_{\partial\Omega_p} k_p \partial_s p_p n_3 q_p = - \int_{x_3=1} k_b \partial_{x_3} p_b q_b \\ + \int_{\omega_p} k_b \partial_{x_3} p_b q_b + \int_{s=-h/2} k_p \partial_s p_p q_p - \int_{s=h/2} k_p \partial_s p_p q_p.$$

By using the boundary condition $\partial_{x_3} p_b = 0$ at $x_3 = 1$, the coupling across the Biot-plate interface $k_p \partial_s p_p|_{\omega_p^+} = k_b \partial_s p_b|_{\omega_p}$, and the coupling across the Stokes-plate interface $w_t - (\mathbf{u} \cdot \mathbf{e}_3)|_{\omega_p} = k_p \partial_s p_p|_{\omega_p^-}$, (3.10) simplifies to

$$(3.11) \quad - \int_0^T \int_{\partial\Omega_b} k_b \nabla p_b \cdot \mathbf{n} q_b - \int_0^T \int_{\partial\Omega_p} k_p \partial_s p_p n_3 q_p = \int_{s=-h/2} (w_t - (\mathbf{u} \cdot \mathbf{e}_3)|_{\omega_p}) q_p.$$

Using the second coupling at the Stokes-plate interface $-\boldsymbol{\sigma}_f\mathbf{e}_3 \cdot \mathbf{e}_3|_{\omega_p} = p_p|_{\omega_p^-}$, we get

$$(3.12) \quad \int_0^T \int_{\omega_p} \boldsymbol{\sigma}_f\mathbf{e}_3 \cdot \mathbf{e}_3|_{\omega_p} z = - \int_0^T \int_{\omega_p} p_p|_{\omega_p^-} z.$$

Last, using again the coupling at the Stokes-plate interface $-\boldsymbol{\sigma}_f\mathbf{e}_3 \cdot \mathbf{e}_3|_{\omega_p} = p_p|_{\omega_p^-}$, the boundary condition $\mathbf{v} = 0$ on $\{x_3 = -1\}$, and the coupling across the plate's middle surface ω_p , $\beta\mathbf{u}|_{\omega_p} \cdot \mathbf{e}_i = -[\boldsymbol{\sigma}_f|_{\omega_p} \mathbf{e}_3] \cdot \mathbf{e}_i$, $i = 1, 2$, we can simplify the boundary term associated with the fluid as follows:

$$(3.13) \quad \int_0^T \int_{\partial\Omega_f} \boldsymbol{\sigma}_f\mathbf{n} \cdot \mathbf{v} = \int_{x_3=-1} \boldsymbol{\sigma}_f\mathbf{e}_3 \cdot \mathbf{v} - \int_{\omega_p} \boldsymbol{\sigma}_f\mathbf{e}_3 \cdot \mathbf{v} \\ = - \int_{\omega_p} [\boldsymbol{\sigma}_f\mathbf{e}_3 \cdot \mathbf{e}_1(\mathbf{v} \cdot \mathbf{e}_1) + \boldsymbol{\sigma}_f\mathbf{e}_3 \cdot \mathbf{e}_2(\mathbf{v} \cdot \mathbf{e}_2) + \boldsymbol{\sigma}_f\mathbf{e}_3 \cdot \mathbf{e}_3(\mathbf{v} \cdot \mathbf{e}_3)] \\ = \int_{\omega_p} \beta(\mathbf{u} \cdot \mathbf{t})(\mathbf{v} \cdot \mathbf{t}) + \int_{\omega_p} p_p|_{\omega_p^-}(\mathbf{v} \cdot \mathbf{e}_3).$$

Combining (3.8) with (3.9), (3.11), (3.12), and (3.13), we obtain that the sum of the boundary terms in the variational form simplifies to

$$I_{\text{bdry}} = -((p_p|_{s=-h/2}, z - \mathbf{v} \cdot \mathbf{e}_3))_{\omega_p} + (\langle w_t - \mathbf{u} \cdot \mathbf{e}_3, q_p|_{s=-h/2} \rangle)_{\omega_p} + \beta((\mathbf{u} \cdot \mathbf{t}, \mathbf{v} \cdot \mathbf{t}))_{\omega_p}.$$

We can now introduce the definition of a weak solution for the fully coupled system. The following weak form applies to all cases of admissible values of ρ_b, ρ_p, c_b, c_p . Namely, the solution and test spaces are built to accommodate subsets of these parameters vanishing.

DEFINITION 1. We say that $(\mathbf{u}, w, p_p, \boldsymbol{\eta}, p_b) \in \mathcal{V}_{\text{sol}}$ is a weak solution to (2.15)–(2.30) if for every test function $(\mathbf{v}, z, q_p, \boldsymbol{\psi}, q_b) \in \mathcal{V}_{\text{test}}$ the following identity holds:

(3.14)

$$\begin{aligned} & -\rho_b((\boldsymbol{\eta}_t, \boldsymbol{\psi}_t))_{\Omega_b} + ((\boldsymbol{\sigma}_b(\boldsymbol{\eta}, p_b), \nabla \boldsymbol{\psi}))_{\Omega_b} - ((c_b p_b + \alpha_b \nabla \cdot \boldsymbol{\eta}, \partial_t q_b))_{\Omega_b} + ((k_b \nabla p_b, \nabla q_b))_{\Omega_b} \\ & - ((c_p p_p - \alpha_p s \Delta w, \partial_t q_p))_{\Omega_p} + ((k_p \partial_s p_p, \partial_s q_p))_{\Omega_p} \\ & - \rho_p((w_t, \partial_t z))_{\omega_p} + D((\Delta w, \Delta z))_{\omega_p} + \alpha_p \left(\left(\int_{-h/2}^{h/2} [s p_p] ds, \Delta z \right) \right)_{\omega_p} + \gamma((w, z))_{\omega_p} \\ & - ((p_p|_{s=-h/2}, z - \mathbf{v} \cdot \mathbf{e}_3))_{\omega_p} + (\langle w_t - \mathbf{u} \cdot \mathbf{e}_3, q_p|_{s=-h/2} \rangle)_{\omega_p} \\ & - \rho_f((\mathbf{u}, \mathbf{v}_t))_{\Omega_f} + \mu_f((\mathbf{D}(\mathbf{u}), \mathbf{D}(\mathbf{v})))_{\Omega_f} + \beta((\mathbf{u} \cdot \mathbf{t}, \mathbf{v} \cdot \mathbf{t}))_{\omega_p} \\ & = \rho_b(\boldsymbol{\eta}_t, \boldsymbol{\psi})|_{t=0} + (c_b p_b + \alpha_b \nabla \cdot \boldsymbol{\eta}, q_b)|_{t=0} + (c_p p_p - \alpha_p s \Delta w, q_p)|_{t=0} \\ & + \rho_p(w_t, z)|_{t=0} + \rho_f(\mathbf{u}, \mathbf{v})|_{t=0} + ((\mathbf{F}_b, \boldsymbol{\psi}))_{\Omega_b} + ((S, q_b))_{\Omega_b} + ((\mathbf{f}, \mathbf{v}))_{\Omega_f}, \end{aligned}$$

where

$$\begin{aligned} \rho_b \boldsymbol{\eta}(\cdot, 0) &= \rho_b \boldsymbol{\eta}^0, \quad \rho_b \boldsymbol{\eta}_t(\cdot, 0) = \rho_b \boldsymbol{\eta}_t^0; \quad \rho_p w(\cdot, 0) = \rho_p w^0, \quad \rho_p w_t(\cdot, 0) = \rho_p w_t^0, \\ c_b p_b(\cdot, 0) + \alpha_b \nabla \cdot \boldsymbol{\eta}(\cdot, 0) &= \zeta_b^0; \quad c_p p_p(\cdot, 0) - \alpha_p \Delta w(\cdot, 0) = \zeta_p^0. \end{aligned}$$

The interpretation of the dual mapping in term $\langle w_t - \mathbf{u} \cdot \mathbf{e}_3, q_p|_{s=-h/2} \rangle_{\omega_p}$ is the following:

- If $\rho_p > 0$, the dual mapping is just the $L^2(0, T; L^2(\omega_p))$ scalar product, which is well defined since by $w_t \in L^2(0, T; L^2(\omega_p))$ (see the definition of the solution space).
- If $\rho_p = 0$, the term is to be interpreted in the following way:

(3.15)

$$\begin{aligned} & (\langle w_t - \mathbf{u} \cdot \mathbf{e}_3, q_p|_{s=-h/2} \rangle)_{\omega_p} \\ & = -((w, \partial_t q_p|_{s=-h/2}))_{\omega_p} - ((\mathbf{u} \cdot \mathbf{e}_3, q_p|_{s=-h/2}))_{\omega_p} + (w, q_p|_{s=-h/2})|_{t=0}. \end{aligned}$$

Remark 3.3. We work in the periodic settings to avoid unnecessary technical difficulties. However, there are some coercivity issues related to this setting. Namely, to ensure coercivity, we require $c_p > 0$. This is because in the degenerate case $c_p = c_b = 0$, the L^2 norm of p_p is not bounded by the energy inequality. More precisely, in the degenerate case the energy estimate provides the bounds for $\|\partial_s p_p\|_{L^2(\Omega_p)}$ and $\|p_p|_{s=-h/2}\|_{H^{-1}((0,T) \times \omega_p \times \{-h/2\})}$, where the latter bound is a consequence of the coupling condition (2.24) and can be proved by taking $(\mathbf{v}, 0, 0, 0, 0)$ as a test function in the weak formulation (1). However, this is not enough to control high oscillations in the x_1 and x_2 direction. For example, we can take $p_p = \sin(\pi n x_1)$ to see that its L^2 norm is not controlled by the energy.

Remark 3.4. Note that conditions of continuity of the elastic displacement and Biot pressure across the Biot-plate interface are included in the definitions of the solution and test spaces. However, the design of finite elements satisfying these constraints can indeed be challenging. One way to address this difficulty is to impose the equality of the traces weakly through Nitsche's method—see, for instance, the original paper [42] and [19] in the context of fluid-structure interactions.

Remark 3.5. We note that the formal energy inequality in (3.1) can be obtained by testing with the solution variable in Definition 1 and considering the subsequent cancellations, presented above.

3.4. Differential formulation from weak form. We note that a strong solution is recovered from a weak solution with sufficient regularity. Indeed, if a weak solution (as in Definition 1) $(\mathbf{u}, w, p_p, \boldsymbol{\eta}, p_b) \in \mathcal{V}_{\text{sol}}$ is sufficiently smooth in space and time, then $(\mathbf{u}, w, p_p, \boldsymbol{\eta}, p_b) \in \mathcal{V}_{\text{sol}}$ satisfies the PDEs (2.15)–(2.17) in a pointwise sense, as well as the coupling conditions (2.19)–(2.24). Reconstruction of the differential formulation proceeds in the following way:

1. Take $\boldsymbol{\psi}$, q_b , z , q_p identically zero on their respective domains in the variational form of Definition 1. Invoke the formal integration by parts with C_c^∞ -test function \mathbf{v} to observe that the Stokes equation is satisfied pointwise a.e. in Ω_f . Then using “standard” test functions \mathbf{v} from the test space $\mathcal{V}_{\text{test}}$, the following integral over ω_p remains:

$$\int_{\omega_p} \left[\boldsymbol{\sigma}_f(\mathbf{u}, p_f) \mathbf{e}_3 \cdot \mathbf{v} + \beta(\mathbf{u} \cdot \mathbf{t})(\mathbf{v} \cdot \mathbf{t}) + p_p|_{s=-h/2} \mathbf{v} \cdot \mathbf{e}_3 \right] = 0.$$

Since \mathbf{v} is arbitrary, we obtain

- (a) the Beavers–Joseph–Saffman condition $\boldsymbol{\sigma}_f \mathbf{n} \cdot \mathbf{t} + \beta \mathbf{u} \cdot \mathbf{t} = 0$ on ω_p , by taking \mathbf{v} to be purely tangential;
 - (b) the pressure condition $p_p|_{s=-h/2} = -\boldsymbol{\sigma}_f \mathbf{e}_3 \cdot \mathbf{e}_3$ on ω_p , by taking $\mathbf{v} = \mathbf{e}_3$.
2. Now take all test function components zero, except z and $\boldsymbol{\psi}$. This gives the coupled dynamic equations for the poroelastic plate displacement w and the Biot displacement $\boldsymbol{\eta}$:

$$\begin{aligned} & -\rho_b((\boldsymbol{\eta}_t, \boldsymbol{\psi}_t))_{\Omega_b} + ((\boldsymbol{\sigma}_b(\boldsymbol{\eta}, p_b), \nabla \boldsymbol{\psi}))_{\Omega_b} - \rho_p((w_t, \partial_t z))_{\omega_p} + D((\Delta w, \Delta z))_{\omega_p} \\ & = \alpha_p \left(\left(\int_{-h/2}^{h/2} [sp_p] ds, \Delta z \right) \right)_{\omega_p} + ((p_p|_{s=-h/2}, z))_{\omega_p} + \rho_b(\boldsymbol{\eta}_t, \boldsymbol{\psi})|_{t=0} \\ & \quad + \rho_p(w_t, z)|_{t=0} + ((\mathbf{F}_b, \boldsymbol{\psi}))_{\Omega_b}. \end{aligned}$$

Similarly as above, to obtain the interior differential equations holding almost everywhere, we use the C_c^∞ test functions and integrate back by parts. Then, by using the standard test functions z and $\boldsymbol{\psi}$ from $\mathcal{V}_{\text{test}}$, after integrating back by parts in the $\boldsymbol{\eta}$ equation, we obtain the boundary terms on the right-hand side given by

$$p_p|_{s=-h/2} + \boldsymbol{\sigma}_b(\boldsymbol{\eta}, p_b) \mathbf{e}_3 \cdot \mathbf{e}_3.$$

Next, we return to the full weak formulation, including the Stokes equation, and take only z , p_p , \mathbf{v} to be different from zero. Undoing the integration by parts in the \mathbf{u} equation gives the trace terms

$$-\boldsymbol{\sigma}_f(\mathbf{u}, p_f) \mathbf{e}_3 \cdot \mathbf{e}_3 + \boldsymbol{\sigma}_b(\boldsymbol{\eta}, p_b) \mathbf{e}_3 \cdot \mathbf{e}_3.$$

Finally, with the interior equations satisfied a.e., we obtain the following identity holding for the interface terms, since the appropriate integral equality holds true for all test functions:

$$p_p|_{s=-h/2} + \boldsymbol{\sigma}_b(\boldsymbol{\eta}, p_b) \mathbf{e}_3 \cdot \mathbf{e}_3 = -\boldsymbol{\sigma}_f(\mathbf{u}, p_f) \mathbf{e}_3 \cdot \mathbf{e}_3 + \boldsymbol{\sigma}_b(\boldsymbol{\eta}, p_b) \mathbf{e}_3 \cdot \mathbf{e}_3.$$

This is exactly the dynamic coupling condition, i.e., the balance of forces acting across the poroelastic plate.

3. Last, let us take $q_p \neq 0$ such that $q_p|_{s=h/2} = 0$, and $q_b = 0$. Again, after integrating by parts and taking into account that the interior equations are satisfied pointwise, the following boundary terms remain:

$$-k_p \int_{\omega_p} \partial_{x_3} p_p|_{s=-h/2} q_p|_{s=-h/2} + \int_{\omega_p} [w_t - \mathbf{u} \cdot \mathbf{e}_3] q_p|_{s=-h/2} = 0.$$

Therefore we obtain $\partial_t w = u_3 + k_p \partial_3 p_p = u_3 - (\mathbf{u}_p)_3$, where $(\mathbf{u}_p)_3$ is the third component of the discharge velocity $\mathbf{u}_p = -k_p \partial_s p_p$, and u_3 is the third component of the Stokes field $\mathbf{u} = (u_1, u_2, u_3)$. This is exactly the kinematic coupling condition at the fluid-poroplate interface.

Note that the remaining “essential” type boundary coupling conditions are built into the compatibility requirements on \mathcal{V}_{sol} and $\mathcal{V}_{\text{test}}$.

4. Statement of main results and proof strategy. In this section we informally state the following two main results of the paper:

1. The existence of a weak solution to the linear evolution problem: in particular, the Biot coefficient (diagonal tensor) k_b is a given function of t and \mathbf{x} . In this case the following parameters are allowed to be nonnegative: $\rho_b, \rho_p, c_b \geq 0$, with only the poroelastic plate’s compressibility parameter $c_p > 0$.
2. The existence of a weak solution to the nonlinear quasi-static problem: the coefficient k_b depends on the solution, in particular on the fluid content $\zeta_b = c_b p + \alpha_b \nabla \cdot \boldsymbol{\eta}$. In this case we consider the quasi-static Biot model, namely, $\rho_b = 0$, with the coefficients $\rho_p, c_b \geq 0$ and $c_p > 0$.

For the main results, we adopt the semidiscretization approach, also known as Rothe’s method, e.g., [54]. In the context of FSI problems, it was developed and used to study moving boundary problems involving linear and nonlinear elastic structures [40, 41]. In the present paper, we extend this approach to deal with FPSI problems, showing that this approach is quite robust and applicable to a large class of FSI problems. Nevertheless, we emphasize that in the present paper, the presence of the thin poroelastic plate is of particular importance, since it serves as a regularizing mechanism [4, 39] in the existence proof, while also allowing perfusion/filtration through the interface.

The proof relies on the following main steps:

1. Construction of approximate solutions.
 - (a) Derive a semidiscrete in time and linearized version of the weak formulation, with the time discretization parameter $[\Delta t] = \frac{T}{N}$. In the semidiscretized formulation, the linearization is performed by evaluating the nonlinear coefficient functions at the previous time step. This defines a sequence of linear elliptic problems for solutions at time $t^n = n[\Delta t]$, with data given at $t^{n-1} = (n-1)[\Delta t]$.
 - (b) Prove existence of a unique solution to the elliptic problem defined for every $n = 1, \dots, N$ by using the Lax–Millgram lemma.
 - (c) Define approximate *solutions*

$$(\mathbf{u}^{[N]}, w^{[N]}, p_p^{[N]}, \boldsymbol{\eta}^{[N]}, p_b^{[N]})$$

as functions that are piecewise constant in time, extrapolating the values obtained from the time discretization and satisfying the approximate weak formulation.

2. Derive uniform estimates in $[\Delta t]$ through appropriate discretized test functions.
3. Obtain weak solution by letting $N \rightarrow \infty$, i.e., $\Delta t \rightarrow 0$, utilizing compactness criteria to push limits on the nonlinear term involving k_b .

Since in steps 1 and 2 we use the linearized problem, these steps are the same for both the linear evolution problem and nonlinear quasi-static problem. However, step 3 deviates, because in the nonlinear case we need to prove additional strong convergence properties. In step 3 we will utilize piecewise constant approximations and an elegant compactness result for piecewise constant approximate solutions [29], which greatly simplifies the construction from past work on nonlinear Biot problems [14, 22, 54].

We begin with a construction of the approximate solutions that covers both cases. Namely, for the linear problem, simply take $k_b \equiv k_b(\mathbf{x}, t)$ as a given function.

Finally, we address uniqueness criteria for solutions that exhibit more regularity than our weak solutions. In particular, the result is of weak-strong uniqueness type, wherein weak solutions from a certain class (see Assumption 5) are unique if there is a single solution in that class exhibiting additional regularity (see Proposition 6.6).

5. Main result I: Linear existence. In this section we consider $k_b = k_b(\mathbf{x}, t) \in L^\infty(0, T; L^\infty(\mathbb{R}))$ as a given function of space and time.

The proof of the existence of a weak solution is based on temporal semidiscretization along with formal energy estimates. It is a direct application of Rothe's method to the coupled linear Stokes–Biot–poroelastic plate problem. We begin by the construction of approximate solutions, given a discretization of the time interval based on a time step Δt .

5.1. Construction of the approximate solutions. Let $[\Delta t] > 0 = T/N$, $N \in \mathbb{N}$. For every fixed N , we inductively define a sequence of approximate solutions $(\mathbf{u}_N^n, w_N^n, (p_p)_N^n, \boldsymbol{\eta}_N^n, (p_b)_N^n)$, $n = 0, \dots, N$. For this purpose, we use an implicit Euler method to discretize the time derivatives, making use of the following notation:

$$(5.1) \quad \dot{\boldsymbol{\eta}}^{n+1} = \frac{\boldsymbol{\eta}^{n+1} - \boldsymbol{\eta}^n}{\Delta t}, \quad \dot{w}^{n+1} = \frac{w^{n+1} - w^n}{\Delta t}.$$

Thus, at every fixed time t^n , we have to “solve” a semidiscretized problem (specified below in (5.6)), with the solution (depending only on the spatial variables) belonging to the following *weak solution space*,

$$(5.2) \quad \mathcal{V}_{\text{sd}} = \left\{ (\mathbf{u}, w, p_p, \boldsymbol{\eta}, p_b) \in V_\# \times H_\#^2(\omega_p) \times H^{0,0,1} \times H_\#^1(\Omega_b) \times H_\#^1(\Omega_b) \right. \\ \left. : p_p|_{s=h/2} = p_b|_{x_3=0}, \boldsymbol{\eta}|_{x_3=0} = w\mathbf{e}_3 \right\},$$

equipped with the following norm,

$$(5.3) \quad \|(\mathbf{u}, w, p_p, \boldsymbol{\eta}, p_b)\|_{\text{sd}}^2 := \|\mathbf{u}\|_{H^1(\Omega_f)}^2 + \|\Delta w\|_{L^2(\omega_p)}^2 + \|w\|_{L^2(\omega_p)}^2 + \|p_p\|_{L^2(\Omega_p)}^2 \\ + \|\partial_s p_p\|_{L^2(\Omega_p)}^2 + \|\boldsymbol{\eta}\|_E^2 + \|\nabla p_b\|_{L^2(\Omega_b)}^2,$$

where we recall that the norm $\|\cdot\|_E$ was defined in (3.1).

LEMMA 5.1. *($\mathcal{V}_{\text{sd}}, \|\cdot\|_{\text{sd}}$) is a Hilbert space. In particular, the norm $\|\cdot\|_{\mathcal{V}_{\text{sd}}}$ defined in (5.3) is equivalent to the usual norm in the space $V_\# \times H_\#^2(\omega_p) \times H^{0,0,1} \times H_\#^1(\Omega_b) \times H_\#^1(\Omega_b)$.*

Proof. We first notice that $\|\Delta w\|_{L^2(\omega_p)} + \|w\|_{L^2(\omega_p)}$ is a norm equivalent to the H^2 norm on $H^2_{\#}(\omega_p)$. This follows by applying elliptic regularity to the case of periodic boundary conditions associated with the operator $-\Delta w + \gamma w \in L^2(\Omega)$, giving full control of the $H^2(\omega_p)$ norm.

Next, we observe that the L^2 norms of $\boldsymbol{\eta}$ and p_b (Biot components) are not included in the definition of $\|\cdot\|_{sd}$, and so we need to show the following Poincaré-type inequalities:

$$(5.4) \quad \|\boldsymbol{\eta}\|_{L^2(\Omega_b)}^2 \leq C\|(\mathbf{u}, w, p_p, \boldsymbol{\eta}, p_b)\|_{sd}^2, \quad \boldsymbol{\eta} \in H^1_{\#}(\Omega_b),$$

$$(5.5) \quad \|p_b\|_{L^2(\Omega_b)}^2 \leq C\|(\mathbf{u}, w, p_p, \boldsymbol{\eta}, p_b)\|_{sd}^2, \quad p_b \in H^1_{\#}(\Omega_b).$$

In contrast with the homogeneous Dirichlet case, the proof of the Poincaré inequalities will follow by employing the interface conditions incorporated in the definition of \mathcal{V}_{sd} . We will prove the inequalities for smooth functions since the general case follows by density argument in the standard way. To prove the first inequality in (5.4) we notice

$$\begin{aligned} |\boldsymbol{\eta}(x_1, x_2, x_3, t)|^2 &= \left| \boldsymbol{\eta}(x_1, x_2, 0, t) + \int_0^{x_3} \partial_{x_3} \boldsymbol{\eta}(x_1, x_2, z, t) dz \right|^2 \\ &\leq C \left(|\boldsymbol{\eta}(x_1, x_2, 0, t)|^2 + \int_0^{x_3} |\partial_{x_3} \boldsymbol{\eta}(x_1, x_2, z, t)|^2 dz \right). \end{aligned}$$

Integrate the above inequality over Ω_b and invoke the interface coupling $\boldsymbol{\eta}|_{\omega_p} = \langle 0, 0, w \rangle$ to obtain

$$\begin{aligned} \|\boldsymbol{\eta}\|_{L^2(\Omega_b)}^2 &\leq C(\|\boldsymbol{\eta}\|_{L^2(\omega_p)}^2 + \|\partial_{x_3} \boldsymbol{\eta}\|_{L^2(\Omega_b)}^2) \\ &\leq C(\|w\|_{L^2(\omega_p)}^2 + \|\boldsymbol{\eta}\|_E^2) \leq C\|(\mathbf{u}, w, p_p, \boldsymbol{\eta}, p_b)\|_{sd}^2. \quad \square \end{aligned}$$

This proves the first inequality.

To prove the second inequality, we first need to estimate the trace of p_b on $x_3 = 0$:

$$p_b^2(x_1, x_2, 0, t) = p_p^2(x_1, x_2, h/2, t) = \left(\frac{2}{h} \int_0^{h/2} \partial_s(sp_p(x_1, x_2, z, t)) dz \right)^2.$$

We continue, as before, by integrating the above equality over ω_p to obtain

$$\|p_b\|_{L^2(\omega_p)}^2 \leq C(\|p_p\|_{L^2(\Omega_p)}^2 + \|\partial_s p_p\|_{L^2(\Omega_p)}^2).$$

Thus, we get

$$\|p_b\|_{L^2(\Omega_b)}^2 \leq C(\|p_b\|_{L^2(\omega_p)}^2 + \|\nabla p_b\|_{L^2(\Omega_b)}^2) \leq C\|(\mathbf{u}, w, p_p, \boldsymbol{\eta}, p_b)\|_{sd}^2.$$

Remark 5.1. If there were homogeneous Dirichlet boundary conditions on any subportion of the boundary for $\boldsymbol{\eta}$ and p_b , the classical Poincaré and Korn inequalities would yield norm equivalences for those variables. In the present configuration, the L^2 control in (5.4) for $\boldsymbol{\eta}$ and p_b is obtained through interface conditions, which gives equivalence of the full norms, as stated in Lemma 5.1.

We now define a weak formulation for the semidiscrete linear problem at time $t^n = n[\Delta t]$ for each $n = 1, \dots, N$. The weak formulation defines semidiscretized approximations of the solution.

DEFINITION 2 (weak formulation for the semidiscrete problem). *The following is the semidiscretized weak formulation of the linear version of problem (2.15)–(2.30) where $k_b^n = k_b(\mathbf{x}, t^n)$:*

Find $(\mathbf{u}^n, w^n, (p_p)^n, \boldsymbol{\eta}^n, (p_b)^n) \in \mathcal{V}_{\text{sd}}$ such that for every $(\mathbf{v}, z, q_p, \boldsymbol{\psi}, q_b) \in \mathcal{V}_{\text{sd}}$ the following holds:

$$\begin{aligned}
 & \rho_b(\dot{\boldsymbol{\eta}}^{n+1} - \dot{\boldsymbol{\eta}}^n, \boldsymbol{\psi})_{\Omega_b} + [\Delta t](\boldsymbol{\sigma}_b(\boldsymbol{\eta}^{n+1}, p_b^{n+1}), \nabla \boldsymbol{\psi})_{\Omega_b} + [\Delta t](c_b \dot{p}_b^{n+1} + \alpha_b \nabla \cdot \dot{\boldsymbol{\eta}}^{n+1}, q_b)_{\Omega_b} \\
 & + [\Delta t](k_b^n \nabla p_b^{n+1}, \nabla q_b)_{\Omega_b} + [\Delta t](c_p \dot{p}_p^{n+1} - \alpha_p s \Delta \dot{w}^{n+1}, q_p)_{\Omega_p} \\
 & + [\Delta t](k_p \partial_s p_p^{n+1}, \partial_s q_p)_{\Omega_p} + \rho_p(\dot{w}^{n+1} - \dot{w}^n, z)_{\omega_p} \\
 & + [\Delta t]D(\Delta w^{n+1}, \Delta z)_{\omega_p} + [\Delta t]\alpha_p \left(\int_{-h/2}^{h/2} [sp_p^{n+1}] ds, \Delta z \right)_{\omega_p} \\
 & + \gamma[\Delta t](w^{n+1}, z)_{\omega_p} - [\Delta t] \left(p_p^{n+1} \Big|_{s=-h/2}, z - \mathbf{v} \cdot \mathbf{e}_3 \right)_{\omega_p} \\
 & + [\Delta t] \left(\dot{w}^{n+1} - \mathbf{u}^{n+1} \cdot \mathbf{e}_3, q_p \Big|_{s=-h/2} \right) \\
 & + \rho_f(\mathbf{u}^{n+1} - \mathbf{u}^n, \mathbf{v})_{\Omega_f} + [\Delta t]\mu_f(\mathbf{D}(\mathbf{u}^{n+1}), \mathbf{D}(\mathbf{v}))_{\Omega_f} + [\Delta t]\beta(\mathbf{u}^{n+1} \cdot \mathbf{t}, \mathbf{v} \cdot \mathbf{t})_{\omega_p} \\
 (5.6) \quad & = [\Delta t](\mathbf{F}_b^{n+1}, \boldsymbol{\psi})_{\Omega_b} + [\Delta t](S^{n+1}, q_b)_{\Omega_b} + [\Delta t](\mathbf{f}^{n+1}, \mathbf{v})_{\Omega_f}
 \end{aligned}$$

with the initial data specified in (2.30) and the discretized time derivative $\dot{\boldsymbol{\eta}}^n$ defined in (5.1).

Notice that in the linear case, k_b^n is the value of $k_b(x, t)$ at the previous time step t^n . In the nonlinear case, we will take $k_b^n = (c_b p_b^n + \alpha_b \nabla \cdot \boldsymbol{\eta}^n)$.

To write this weak formulation entirely in terms of the unknown functions $(\mathbf{u}^n, w^n, (p_p)^n, \boldsymbol{\eta}^n, (p_b)^n)$ belonging to the function space \mathcal{V}_{sd} , we express the terms $\dot{\boldsymbol{\eta}}^n$ and $\dot{\boldsymbol{\eta}}^{n+1}$ in terms of $\boldsymbol{\eta}$ using (5.1) to obtain

$$\begin{aligned}
 (5.7) \quad & \rho_b(\boldsymbol{\eta}^{n+1}, \boldsymbol{\psi})_{\Omega_b} + [\Delta t]^2(\boldsymbol{\sigma}_b(\boldsymbol{\eta}^{n+1}, p_b^{n+1}), \nabla \boldsymbol{\psi})_{\Omega_b} + [\Delta t](c_b p_b^{n+1}, q_b)_{\Omega_b} \\
 & + [\Delta t](\alpha_b \nabla \boldsymbol{\eta}^{n+1}, q_b)_{\Omega_b} + [\Delta t]^2(k_b^n \nabla p_b^{n+1}, \nabla q_b)_{\Omega_b} + [\Delta t](c_p p_p^{n+1} \\
 & - \alpha_p s \Delta w^{n+1}, q_p)_{\Omega_p} + [\Delta t]^2(k_p \partial_s p_p^{n+1}, \partial_s q_p)_{\Omega_p} + \rho_p(w^{n+1}, z)_{\omega_p} \\
 & + [\Delta t]^2 D(\Delta w^{n+1}, \Delta z)_{\omega_p} + [\Delta t]^2 \alpha_p \left(\int_{-h/2}^{h/2} [sp_p^{n+1}] ds, \Delta z \right)_{\omega_p} + \gamma[\Delta t]^2(w^{n+1}, z)_{\omega_p} \\
 & - [\Delta t]^2 \left(p_p^{n+1} \Big|_{s=-h/2}, z \right)_{\omega_p} + [\Delta t]^2 \left(p_p^{n+1} \Big|_{s=-h/2}, \mathbf{v} \cdot \mathbf{e}_3 \right)_{\omega_p} \\
 & + [\Delta t] \left(w^{n+1}, q_p \Big|_{s=-h/2} \right) - [\Delta t]^2 \left(\mathbf{u}^{n+1} \cdot \mathbf{e}_3, q_p \Big|_{s=-h/2} \right) \\
 & + [\Delta t]\rho_f(\mathbf{u}^{n+1}, \mathbf{v})_{\Omega_f} + [\Delta t]^2\mu_f(\mathbf{D}(\mathbf{u}^{n+1}), \mathbf{D}(\mathbf{v}))_{\Omega_f} + [\Delta t]^2\beta(\mathbf{u}^{n+1} \cdot \mathbf{t}, \mathbf{v} \cdot \mathbf{t})_{\omega_p} \\
 & = [\Delta t]^2(\mathbf{F}_b^{n+1}, \boldsymbol{\psi})_{\Omega_b} + [\Delta t]^2(S^{n+1}, q_b)_{\Omega_b} + [\Delta t]^2(\mathbf{f}^{n+1}, \mathbf{v})_{\Omega_f} + [\Delta t](\dot{\boldsymbol{\eta}}^n, \boldsymbol{\psi})_{\Omega_b} \\
 & + [\Delta t](\dot{w}^n, z)_{\omega_p} + [\Delta t]\rho_f(\mathbf{u}^n, \mathbf{v})_{\Omega_f} + \rho_b(\boldsymbol{\eta}^n, \boldsymbol{\psi})_{\Omega_b} + [\Delta t](c_b p_b^n + \alpha_b \nabla \boldsymbol{\eta}^n, q_b)_{\Omega_b} \\
 & + [\Delta t](c_p p_p^n - \alpha_p s \Delta w^n, q_p)_{\Omega_p} + \rho_p(w^n, z)_{\omega_p} + [\Delta t] \left(w^n, q_p \Big|_{s=-h/2} \right).
 \end{aligned}$$

We note that the above problem, although equivalent to the discrete weak form in (5.6), does not have a coercive structure. This is a consequence of the particular

coupling in our multilayer problem and the use of a mixed-velocity/solution test functions in obtaining the energy estimates. To circumvent this issue, we modify the test functions (i.e., the variational problem we are trying to solve) in the following way:

$$(5.8) \quad q_b \mapsto [\Delta t]q_b; \quad q_p \mapsto [\Delta t]q_p; \quad \mathbf{v} \mapsto [\Delta t]\mathbf{v}.$$

This rescaling can be undone, of course. This is because the rescaling of test functions does not affect the admissibility in the space \mathcal{V}_{sd} , and, after the use of the Lax–Milgram lemma to obtain existence, as described below, the variational problem in (5.7) is recovered through the “for all” quantifier in the definition of a weak solution. As a consequence, the solution to (5.7) recovers the solution to the original semidiscretized problem (5.6).

With the rescaled test functions (5.8), the weak formulation of the semidiscretized linear problem is given by the following.

DEFINITION 3 (weak formulation with rescaled test functions). *We say that a function $(\mathbf{u}^n, w^n, (p_p)^n, \boldsymbol{\eta}^n, (p_b)^n) \in \mathcal{V}_{\text{sd}}$ is a weak solution to the semidiscretized linear problem (2.15)–(2.30) if for every test function $([\Delta t]\mathbf{v}, z, [\Delta t]q_p, \boldsymbol{\psi}, [\Delta t]q_b) \in \mathcal{V}_{\text{sd}}$ the following holds:*

$$(5.9) \quad \begin{aligned} & \rho_b(\boldsymbol{\eta}^{n+1}, \boldsymbol{\psi})_{\Omega_b} + [\Delta t]^2(\boldsymbol{\sigma}_b(\boldsymbol{\eta}^{n+1}, p_b^{n+1}), \nabla \boldsymbol{\psi})_{\Omega_b} \\ & + [\Delta t](c_b p_b^{n+1}, [\Delta t]q_b)_{\Omega_b} + [\Delta t](\alpha_b \nabla \boldsymbol{\eta}^{n+1}, [\Delta t]q_b)_{\Omega_b} + [\Delta t]^2(k_b^n \nabla p_b^{n+1}, [\Delta t] \nabla q_b)_{\Omega_b} \\ & + [\Delta t](c_p p_p^{n+1} - \alpha_p s \Delta w^{n+1}, [\Delta t]q_p)_{\Omega_p} + [\Delta t]^2(k_p \partial_s p_p^{n+1}, [\Delta t] \partial_s q_p)_{\Omega_p} + \rho_p(w^{n+1}, z)_{\omega_p} \\ & + [\Delta t]^2 D(\Delta w^{n+1}, \Delta z)_{\omega_p} + [\Delta t]^2 \alpha_p \left(\int_{-h/2}^{h/2} [s p_p^{n+1}] ds, \Delta z \right)_{\omega_p} + \gamma [\Delta t]^2 (w^{n+1}, z)_{\omega_p} \\ & - [\Delta t]^2 \left(p_p^{n+1} \Big|_{s=-h/2}, z \right)_{\omega_p} + [\Delta t]^2 \left(p_p^{n+1} \Big|_{s=-h/2}, [\Delta t] \mathbf{v} \cdot \mathbf{e}_3 \right)_{\omega_p} \\ & + [\Delta t] \left(w^{n+1}, [\Delta t]q_p \Big|_{s=-h/2} \right) - [\Delta t]^2 \left(\mathbf{u}^{n+1} \cdot \mathbf{e}_3, [\Delta t]q_p \Big|_{s=-h/2} \right) \\ & + [\Delta t] \left[[\Delta t] \rho_f(\mathbf{u}^{n+1}, \mathbf{v})_{\Omega_f} + [\Delta t]^2 \mu_f(\mathbf{D}(\mathbf{u}^{n+1}), \mathbf{D}(\mathbf{v}))_{\Omega_f} + [\Delta t]^2 \beta(\mathbf{u}^{n+1} \cdot \mathbf{t}, \mathbf{v} \cdot \mathbf{t})_{\omega_p} \right] \\ & = [\Delta t]^2(\mathbf{F}_b^{n+1}, \boldsymbol{\psi})_{\Omega_b} + [\Delta t]^2(S^{n+1}, [\Delta t]q_b)_{\Omega_b} + [\Delta t]^2(\mathbf{f}^{n+1}, [\Delta t]\mathbf{v})_{\Omega_f} \\ & + [\Delta t](\boldsymbol{\eta}^n, \boldsymbol{\psi})_{\Omega_b} + [\Delta t](\dot{w}^n, z)_{\omega_p} + [\Delta t]\rho_f(\mathbf{u}^n, [\Delta t]\mathbf{v})_{\Omega_f} + \rho_b(\boldsymbol{\eta}^n, \boldsymbol{\psi})_{\Omega_b} + \rho_p(w^n, z)_{\omega_p} \\ & + [\Delta t](c_b p_b^n + \alpha_b \nabla \boldsymbol{\eta}^n, [\Delta t]q_b)_{\Omega_b} + [\Delta t](c_p p_p^n - \alpha_p s \Delta w^n, [\Delta t]q_p)_{\Omega_p} \\ & + [\Delta t] \left(w^n, [\Delta t]q_p \Big|_{s=-h/2} \right) \end{aligned}$$

with the initial data specified in (2.30).

We aim at using the Lax–Milgram lemma to prove the existence of a weak solution specified in Definition 3. More precisely, we will prove the following result.

THEOREM 5.2. *There exists a unique weak solution to (5.9).*

To prove this result using a Lax–Milgram approach we introduce a bilinear form on \mathcal{V}_{sd} , associated with the left-hand side of (5.9), defining our elliptic operator, and a functional on \mathcal{V}_{sd} associated with the right-hand side of (5.9) given in terms

of $\boldsymbol{\eta}^n, \dot{\boldsymbol{\eta}}^n, w^n, \dot{w}^n, \mathbf{u}^n, p_b^n, p_p^n$ and the source terms $\mathbf{F}_b^{n+1}, S^{n+1}, \mathbf{f}^{n+1}$, treated as given data.

More precisely, given k_b^n , we introduce a bilinear form $a_n(\cdot, \cdot)$ on $\mathcal{V}_{\text{sd}} \times \mathcal{V}_{\text{sd}}$ as

$$\begin{aligned}
 (5.10) \quad a_n & \left((\boldsymbol{\eta}^{n+1}, p_b^{n+1}, w^{n+1}, p_p^{n+1}, \mathbf{u}^{n+1}), (\boldsymbol{\psi}, q_b, z, q_p, \mathbf{v}) \right) \\
 & := \rho_b(\boldsymbol{\eta}^{n+1}, \boldsymbol{\psi})_{\Omega_b} + [\Delta t]^2 (\boldsymbol{\sigma}_b(\boldsymbol{\eta}^{n+1}, p_b^{n+1}), \nabla \boldsymbol{\psi})_{\Omega_b} \\
 & \quad + [\Delta t]^2 (c_b p_b^{n+1}, q_b)_{\Omega_b} + [\Delta t]^2 (\alpha_b \nabla \boldsymbol{\eta}^{n+1}, q_b)_{\Omega_b} + [\Delta t]^3 (k_b^n \nabla p_b^{n+1}, \nabla q_b)_{\Omega_b} \\
 & \quad + [\Delta t]^2 (c_p p_p^{n+1} - \alpha_p s \Delta w^{n+1}, q_p)_{\Omega_p} + [\Delta t]^3 (k_p \partial_s p_p^{n+1}, \partial_s q_p)_{\Omega_p} + \rho_p (w^{n+1}, z)_{\omega_p} \\
 & \quad + [\Delta t]^2 D(\Delta w^{n+1}, \Delta z)_{\omega_p} + \gamma [\Delta t]^2 (w^{n+1}, z)_{\omega_p} + [\Delta t]^2 \alpha_p \left(\int_{-h/2}^{h/2} [s p_p^{n+1}] ds, \Delta z \right)_{\omega_p} \\
 & \quad - [\Delta t]^2 \left(p_p^{n+1} \Big|_{s=-h/2}, z \right)_{\omega_p} + [\Delta t]^3 \left(p_p^{n+1} \Big|_{s=-h/2}, \mathbf{v} \cdot \mathbf{e}_3 \right)_{\omega_p} \\
 & \quad + [\Delta t]^2 \left(w^{n+1}, q_p \Big|_{s=-h/2} \right) - [\Delta t]^3 \left(\mathbf{u}^{n+1} \cdot \mathbf{e}_3, q_p \Big|_{s=-h/2} \right) \\
 & \quad + [\Delta t]^2 \rho_f(\mathbf{u}^{n+1}, \mathbf{v})_{\Omega_f} + [\Delta t]^3 \mu_f(\mathbf{D}(\mathbf{u}^{n+1}), \mathbf{D}(\mathbf{v}))_{\Omega_f} + [\Delta t]^3 \beta(\mathbf{u}^{n+1} \cdot \mathbf{t}, \mathbf{v} \cdot \mathbf{t})_{\omega_p}.
 \end{aligned}$$

Notice again that the dependence of the bilinear form $a_n(\cdot, \cdot)$ on n comes specifically through the linear coefficient k_b^n in the case when this function exhibits any temporal dependence.

Similarly, we introduce the functional \mathcal{F}_n by

$$\begin{aligned}
 (5.11) \quad \mathcal{F}_n & (\boldsymbol{\psi}, q_b, z, q_p, \mathbf{v}) := [\Delta t]^2 (\mathbf{F}_b^{n+1}, \boldsymbol{\psi})_{\Omega_b} + [\Delta t]^3 (S^{n+1}, q_b)_{\Omega_b} + [\Delta t]^3 (\mathbf{f}^{n+1}, \mathbf{v})_{\Omega_f} \\
 & \quad + [\Delta t] (\dot{\boldsymbol{\eta}}^n, \boldsymbol{\psi})_{\Omega_b} + [\Delta t] (\dot{w}^n, z)_{\omega_p} + [\Delta t]^2 \rho_f(\mathbf{u}^n, \mathbf{v})_{\Omega_f} \\
 & \quad + \rho_b(\boldsymbol{\eta}^n, \boldsymbol{\psi})_{\Omega_b} + [\Delta t]^2 (c_b p_b^n \\
 & \quad + \alpha_b \nabla \boldsymbol{\eta}^n, q_b)_{\Omega_b} + [\Delta t]^2 (c_p p_p^n - \alpha_p s \Delta w^n, q_p)_{\Omega_p} \\
 & \quad + \rho_p(w^n, z)_{\omega_p} + [\Delta t]^2 \left(w^n, q_p \Big|_{s=-h/2} \right),
 \end{aligned}$$

which depends on $[\Delta t]$, the source terms $\mathbf{F}_b, S, \mathbf{f}$ at t^{n+1} , and a solution evaluated at the previous time step t^n .

We have the following lemma.

LEMMA 5.3. *Suppose that $c_p > 0$ and $\rho_b, \rho_p, c_b \geq 0$. Consider $a_n : \mathcal{V}_{\text{sd}} \times \mathcal{V}_{\text{sd}} \rightarrow \mathbb{R}$ and $\mathcal{F}_n \in \mathcal{L}(\mathcal{V}_{\text{sd}}, \mathbb{R})$, as defined in (5.10) and (5.11) above. Then, as a bilinear form, $a_n(\cdot, \cdot)$ is continuous and coercive, and $\mathcal{F}_n \in [\mathcal{V}_{\text{sd}}]'$.*

Notice that in using Lax–Milgram with our particular rescaling, the setup is robust in that it allows c_b, ρ_b, ρ_p to vanish.

Proof. First we demonstrate the coercivity of $a_n(\cdot, \cdot)$ on $\mathcal{V}_{\text{sd}} \times \mathcal{V}_{\text{sd}}$. We choose $\psi = \boldsymbol{\eta}^{n+1}$, $q_b = p_b^{n+1}$, $q_p = p_p^{n+1}$, and $\mathbf{v} = \mathbf{u}^{n+1}$ and calculate

$$\begin{aligned} a_n(\mathbf{u}^{n+1}, w^{n+1}, p_p^{n+1}, \boldsymbol{\eta}^{n+1}, p_b^{n+1}), (\mathbf{u}^{n+1}, w^{n+1}, p_p^{n+1}, \boldsymbol{\eta}^{n+1}, p_b^{n+1})) \\ = \rho_b \|\boldsymbol{\eta}^{n+1}\|_{\Omega_b}^2 + [\Delta t]^2 \|\boldsymbol{\eta}^{n+1}\|_E^2 - [\Delta t]^2 \alpha_b(p_b^{n+1}, \nabla \boldsymbol{\eta}^{n+1})_{\Omega_b} \\ + [\Delta t]^2 (\alpha_b \nabla \boldsymbol{\eta}^{n+1}, p_b^{n+1})_{\Omega_b} + [\Delta t]^2 c_b \|p_b^{n+1}\|_{\Omega_b}^2 + [\Delta t]^3 \|(k_b^n)^{1/2} \nabla p_b^{n+1}\|_{\Omega_b}^2 \\ + [\Delta t]^2 c_p \|p_p^{n+1}\|_{\Omega_p}^2 - [\Delta t]^2 \alpha_p(s \Delta w^{n+1}, p_p^{n+1})_{\Omega_p} + [\Delta t]^3 \|k_p^{1/2} \partial_s p_p^{n+1}\|_{\Omega_p}^2 \\ + \rho_p \|w^{n+1}\|_{\omega_p}^2 + [\Delta t]^2 D \|\Delta w^{n+1}\|_{\omega_p}^2 + \gamma [\Delta t]^2 \|w^{n+1}\|_{\omega_p}^2 \\ + [\Delta t]^2 \alpha_p \left(\int_{-h/2}^{h/2} [s p_p^{n+1}] ds, \Delta w^{n+1} \right)_{\omega_p} - [\Delta t]^2 \left(p_p^{n+1} \Big|_{s=-h/2}, w^{n+1} \right)_{\omega_p} \\ + [\Delta t]^3 \left(p_p^{n+1} \Big|_{s=-h/2}, \mathbf{u}^{n+1} \cdot \mathbf{e}_3 \right)_{\omega_p} + [\Delta t]^2 \left(w^{n+1}, p_p^{n+1} \Big|_{s=-h/2} \right) \\ - [\Delta t]^3 \left(\mathbf{u}^{n+1} \cdot \mathbf{e}_3, p_p^{n+1} \Big|_{s=-h/2} \right) + [\Delta t]^2 \rho_f (\mathbf{u}^{n+1}, \mathbf{u}^{n+1})_{\Omega_f} \\ + [\Delta t]^3 \mu_f (\mathbf{D}(\mathbf{u}^{n+1}), \mathbf{D}(\mathbf{u}^{n+1}))_{\Omega_f} + [\Delta t]^3 \beta (\mathbf{u}^{n+1} \cdot \mathbf{t}, \mathbf{u}^{n+1} \cdot \mathbf{t})_{\omega_p}. \end{aligned}$$

Now, because of the correct scalings in terms of $[\Delta t]$, we can cancel out both Biot type mixed terms, as well as boundary coupling terms, to obtain

$$\begin{aligned} a_n(\mathbf{u}^{n+1}, w^{n+1}, p_p^{n+1}, \boldsymbol{\eta}^{n+1}, p_b^{n+1}), (\mathbf{u}^{n+1}, w^{n+1}, p_p^{n+1}, \boldsymbol{\eta}^{n+1}, p_b^{n+1})) \\ = \rho_b \|\boldsymbol{\eta}^{n+1}\|_{\Omega_b}^2 + [\Delta t]^2 \|\boldsymbol{\eta}^{n+1}\|_E^2 + [\Delta t]^2 c_b \|p_b^{n+1}\|_{\Omega_b}^2 + [\Delta t]^3 \|[k_b^n]^{1/2} \nabla p_b^{n+1}\|_{\Omega_b}^2 \\ + [\Delta t]^2 c_p \|p_p^{n+1}\|_{\Omega_p}^2 + [\Delta t]^3 \|[k_p^n]^{1/2} \partial_s p_p^{n+1}\|_{\Omega_p}^2 + \rho_p \|w^{n+1}\|_{\omega_p}^2 \\ + [\Delta t]^2 D \|\Delta w^{n+1}\|_{\omega_p}^2 + \gamma [\Delta t]^2 \|w^{n+1}\|_{\omega_p}^2 + [\Delta t]^2 \|\mathbf{u}^{n+1}\|_{\Omega_f}^2 \\ + [\Delta t]^3 \mu_f \|\mathbf{D}(\mathbf{u}^{n+1})\|_{\Omega_f}^2 + [\Delta t]^3 \beta \|\mathbf{u}^{n+1} \cdot \mathbf{t}\|_{\omega_p}^2. \end{aligned}$$

We can now estimate the right-hand side to obtain coercivity on \mathcal{V}_{sd} :

$$\begin{aligned} a_n(\mathbf{u}^{n+1}, w^{n+1}, p_p^{n+1}, \boldsymbol{\eta}^{n+1}, p_b^{n+1}), (\mathbf{u}^{n+1}, w^{n+1}, p_p^{n+1}, \boldsymbol{\eta}^{n+1}, p_b^{n+1})) \\ \gtrsim [\Delta t]^2 \|\boldsymbol{\eta}^{n+1}\|_{\mathbf{H}^1(\Omega_b)}^2 + [\Delta t]^3 \|p_b^{n+1}\|_{H^1(\Omega_b)}^2 + [\Delta t]^3 \|p_p^{n+1}\|_{H^1(\Omega_p)}^2 \\ + [\Delta t]^2 \|w^{n+1}\|_{H^2(\omega_p)}^2 + [\Delta t]^3 \|\mathbf{u}^{n+1}\|_{\mathbf{H}^1(\Omega_f)}^2 \\ \gtrsim \min([\Delta t]^2, [\Delta t]^3) \|\mathbf{u}^{n+1}, w^{n+1}, p_p^{n+1}, \boldsymbol{\eta}^{n+1}, p_b^{n+1}\|_{\mathcal{V}_{\text{sd}}}^2. \end{aligned}$$

Here, we have implicitly used the lower bound $k_b(\mathbf{x}, t) \geq k_{\min} > 0$, and the notation \gtrsim , which represents a bound by a generic constant depending on $\rho_f, \rho_b, c_b, \alpha_b, c_p, \alpha_p, \rho_p$, as well as the Korn's and Poincaré constants, and possibly $[\Delta t]$.

This estimate shows coercivity for the variable $(\mathbf{u}^{n+1}, w^{n+1}, p_p^{n+1}, \boldsymbol{\eta}^{n+1}, p_b^{n+1})$ in the \mathcal{V}_{sd} norm. The quantities $\dot{\boldsymbol{\eta}}^{n+1}$ and \dot{w}^{n+1} are recovered from the formulae in (5.1), recalling that $\boldsymbol{\eta}^n \in \mathbf{L}^2(\Omega_b)$ and $w^n \in L^2(\omega_p)$ are given as data.

To see that the functional \mathcal{F}_n belongs to $[\mathcal{V}_{sd}]'$ we derive a straightforward estimate in terms of L^2 norms:

$$\begin{aligned} \|\mathcal{F}\|_{[\mathcal{V}_{sd}]'} &\lesssim [\Delta t]^2 [\|\mathbf{F}_b^{n+1}\|_{\Omega_b} + [\Delta t]\|S^{n+1}\|_{\Omega_b} + [\Delta t]\|\mathbf{f}^{n+1}\|_{\Omega_f}] \\ &\quad + [\Delta t] [\|\boldsymbol{\eta}^n\|_{\Omega_b} + \|\dot{w}^n\|_{\omega_p} + [\Delta t]\|\mathbf{u}^n\|_{\Omega_f}] \\ &\quad + [\Delta t]^2 [\|p_b^n\|_{\Omega_b} + \|\boldsymbol{\eta}^n\|_E + \|p_p^n\|_{\Omega_p} + \|\Delta w^n\|_{\omega_p}] \\ &\quad + \|\boldsymbol{\eta}^n\|_{\Omega_b} + \|w^n\|_{\omega_p}. \end{aligned} \quad \square$$

The proof of Theorem 5.2 now follows by applying the Lax–Milgram lemma to the problem

$$\begin{aligned} a_n((\mathbf{u}^{n+1}, w^{n+1}, p_p^{n+1}, \boldsymbol{\eta}^{n+1}, p_b^{n+1}), (\boldsymbol{\psi}, q_b, z, q_p, \mathbf{v})) \\ = \mathcal{F}_n(\boldsymbol{\psi}, q_b, z, q_p, \mathbf{v}), \quad \forall (\boldsymbol{\psi}, q_b, z, q_p, \mathbf{v}) \in \mathcal{V}_{sd}, \end{aligned}$$

defined on the Hilbert space \mathcal{V}_{sd} .

We emphasize that the approximate solution lies in the test space, as is necessary for obtaining estimates later on.

Remark 5.2. We note that in the above construction, the continuity and coercivity constants may depend on $[\Delta t]$ in a singular way. However, we utilize the Lax–Milgram lemma only for the existence of an approximate solution to the re-scaled problem (5.9). After obtaining the solution at the time t^{n+1} from the data at t^n , we recover the solution to the original problem (5.6). Once we have the solution to (5.6), we obtain a priori estimates for problem (5.6). We note that the approximate solution lies in the test space, which will be important for the choice of appropriate multipliers in the derivation of a priori estimates. The resulting bounds will be uniform in $[\Delta t]$. This feature is present in the related considerations [14, 16, 54].

Theorem 5.2 provides a sequence of approximate functions, which are functions of the spatial variable only, defined for every $t^n, n = 0, \dots, N$. To define *approximate solutions* we extend these functions to the entire time interval $[0, T]$ by extrapolation as piecewise constant functions in time, to obtain the following *approximate solutions*:

$$\begin{aligned} (5.12) \quad &(\mathbf{u}^{[N]}, w^{[N]}, p_p^{[N]}, \boldsymbol{\eta}^{[N]}, p_b^{[N]})(t) \\ &= (\mathbf{u}_N^n, w_N^n, (p_p)_N^n, \boldsymbol{\eta}_N^n, (p_b)_N^n), \quad t \in (t^{n-1}, t^n], \quad n = 1, \dots, N. \end{aligned}$$

Since we will have to work with derivatives of approximate functions, we introduce the following definition.

DEFINITION 4. For a piecewise constant function $f^{[N]}$, the time derivative of $f^{[N]}$ is a function denoted by $\dot{f}^{[N]}(t)$, defined via backward difference quotients:

$$(5.13) \quad \dot{f}^{[N]}(t) = \frac{f_N^n - f_N^{n-1}}{[\Delta t]}, \quad t \in (t^{n-1}, t^n].$$

With this notion of the time derivative, one can easily see that the approximate solutions satisfy the following weak formulation.

PROPOSITION 5.4. The approximate solutions $(\mathbf{u}^{[N]}, w^{[N]}, p_p^{[N]}, \boldsymbol{\eta}^{[N]}, p_b^{[N]})$, defined by (5.12), satisfy the following weak formulation for all test functions $(\mathbf{v}, z, q_p, \boldsymbol{\psi}, q_b) \in$

\mathcal{V}_{test} :

(5.14)

$$\begin{aligned} & \rho_b((\ddot{\boldsymbol{\eta}}^{[N]}, \boldsymbol{\psi}))_{\Omega_b} + ((\boldsymbol{\sigma}_b(\boldsymbol{\eta}^{[N]}, p_b^{[N]}), \nabla \boldsymbol{\psi}))_{\Omega_b} + ((c_b \dot{p}_b^{[N]} + \alpha_b \nabla \cdot \dot{\boldsymbol{\eta}}^{[N]}, q_b))_{\Omega_b} \\ & + ((k_b(\tau_{\Delta t}(c_b p_b^{[N]} + \alpha_b \nabla \cdot \boldsymbol{\eta}^{[N]}) \nabla p_b^{[N]}, \nabla q_b))_{\Omega_b} + ((c_p \dot{p}_p^{[N]} - \alpha_p s \Delta \dot{w}^{[N]}, q_p))_{\Omega_p} \\ & + ((k_p \partial_s p_p^{[N]}, \partial_s q_p))_{\Omega_p} + \rho_p((\ddot{w}^{[N]}, z))_{\omega_p} + D((\Delta w^{[N]}, \Delta z))_{\omega_p} \\ & + \alpha_p \left(\left(\int_{-h/2}^{h/2} [s p_p^{[N]}] ds, \Delta z \right) \right)_{\omega_p} - \left(\left(p_p^{[N]} \Big|_{s=-h/2}, z - \mathbf{v} \cdot \mathbf{e}_3 \right) \right)_{\omega_p} \\ & + \left(\left(\dot{w}^{[N]} - \mathbf{u}^{[N]} \cdot \mathbf{e}_3, q_p \Big|_{s=-h/2} \right) \right) + \rho_f((\dot{\mathbf{u}}^{[N]}, \mathbf{v}))_{\Omega_f} \\ & + \mu_f((\mathbf{D}(\mathbf{u}^{[N]}), \mathbf{D}(\mathbf{v})))_{\Omega_f} + \beta(\mathbf{u}^{[N]} \cdot \mathbf{t}, \mathbf{v} \cdot \mathbf{t})_{\omega_p} \\ & = ((\mathbf{F}_b^{[N]}, \boldsymbol{\psi}))_{\Omega_b} + ((S^{[N]}, q_b))_{\Omega_b} + ((\mathbf{f}^{[N]}, \mathbf{v}))_{\Omega_f}, \end{aligned}$$

where $\tau_{\Delta t}$ is the translation operator defined by $\tau_{\Delta t} f = f(t - \Delta t)$.

To see that this is true, we first focus on the time interval (t^n, t^{n+1}) and the weak formulation (5.6). Let $(\mathbf{v}, z, q_p, \boldsymbol{\psi}, q_b) \in \mathcal{V}_{test}$, where \mathcal{V}_{test} is defined by (3.2). Notice that $(\mathbf{v}, z, q_p, \boldsymbol{\psi}, q_b)(t)$ for $t \in (t^n, t^{n+1})$ is an admissible test function for the weak formulation (5.6). Thus, take it as a test function in (5.6), integrate the resulting formulation in time from t^n to t^{n+1} , and then sum with respect to $n = 1, \dots, N$, to obtain that the approximate solutions satisfy the approximate weak form (5.14).

5.2. Uniform a priori estimates for the approximate solutions. We show here that the following estimates, uniform in $[\Delta t]$, or equivalently, independent of N , hold for approximate solutions.

LEMMA 5.5. *There exists a constant $C > 0$, independent of N , such that approximate solutions $\mathbf{u}^{[N]}, w^{[N]}, p_p^{[N]}, \boldsymbol{\eta}^{[N]}, p_b^{[N]}$ satisfy the following estimates:*

$$\begin{aligned} & \rho_f \|\mathbf{u}^{[N]}\|_{L_t^\infty L_x^2}^2 + \rho_p \|\dot{w}^{[N]}\|_{L_t^\infty L_x^2}^2 + \rho_b \|\dot{\boldsymbol{\eta}}^{[N]}\|_{L_t^\infty L_x^2}^2 \leq C, \\ & c_p \|p_p^{[N]}\|_{L_t^\infty L_x^2}^2 + \|\boldsymbol{\eta}^{[N]}\|_{L_t^\infty E} + c_b \|p_b^{[N]}\|_{L_t^\infty L_x^2}^2 + D \|\Delta w^{[N]}\|_{L_t^\infty L_x^2}^2 \leq C, \\ & \mu_f \|\mathbf{D}(\mathbf{u}^{[N]})\|_{L_t^2 L_x^2}^2 + \beta \|\mathbf{u}^{[N]} \cdot \mathbf{t}\|_{L_t^2 L_x^2(\omega_p)}^2 + \|\partial_{x_3} p_p^{[N]}\|_{L_t^2 L_x^2}^2 + \|\nabla p_b^{[N]}\|_{L_t^2 L_x^2}^2 \leq C. \end{aligned}$$

The shorthand notation $L_t^2 L_x^2$, for instance, indicates the space $L^2(0, T; L^2(\Omega))$.

Proof. To simplify notation, in this proof we will be assuming that all the physical constants are equal to 1, except for the constants c_p, c_b, ρ_p, ρ_b , which can vanish (in the quasistatic case).

We start by obtaining an a priori estimate on the functions $\mathbf{u}^n, w^n, (p_p)^n, \boldsymbol{\eta}^n, (p_b)^n$, satisfying the semidiscretized problem (5.6). For this purpose, we use the following test functions in (5.6): $\boldsymbol{\psi} = \dot{\boldsymbol{\eta}}^{n+1}$, $q_b = p_b^{n+1}$, $q_p = p_p^{n+1}$, $z = \dot{w}^{n+1}$ and $\mathbf{v} = \mathbf{u}^{n+1}$. Using Young's inequality and absorbing all constants that do not depend on $[\Delta t]$ we

get

$$\begin{aligned}
& \rho_b \|\dot{\boldsymbol{\eta}}^{n+1}\|_{\Omega_b}^2 + [\Delta t](\sigma^E(\boldsymbol{\eta}^{n+1}), \nabla \dot{\boldsymbol{\eta}}^{n+1})_{\Omega_b} + c_b[\Delta t](\dot{p}_b^{n+1}, p_b^{n+1})_{\Omega_b} \\
& + [\Delta t]\|(k_b^n)^{1/2} \nabla p_b^{n+1}\|_{\Omega_b}^2 + c_p[\Delta t](\dot{p}_p^{n+1}, p_p^{n+1})_{\Omega_p} + [\Delta t]\|k_p^{1/2} \partial_s p_p^{n+1}\|_{\Omega_p}^2 \\
& + \rho_p \|\dot{w}^{n+1}\|_{\omega_p}^2 + [\Delta t](\Delta w^{n+1}, \Delta \dot{w}^{n+1})_{\omega_p} + \|\mathbf{u}^{n+1}\|_{\Omega_f}^2 + [\Delta t]\|\mathbf{D}(\mathbf{u}^{n+1})\|_{\Omega_f}^2 \\
& + [\Delta t]\|\mathbf{u}^{n+1} \cdot \mathbf{t}\|_{\omega_p}^2 \\
& \lesssim \rho_b \|\dot{\boldsymbol{\eta}}^n\|_{\Omega_b}^2 + \rho_p \|\dot{w}^n\|_{\omega_p}^2 + \|\mathbf{u}^n\|_{\Omega_f}^2 + [\Delta t]\|\mathbf{F}_b^{n+1}\|_{\Omega_b}^2 + [\Delta t]\|S^{n+1}\|_{\Omega_b}^2 + [\Delta t]\|\mathbf{f}^{n+1}\|_{\Omega_f}^2.
\end{aligned}$$

By invoking the definition of difference quotients, as well as Young's inequality, we obtain the following a priori estimate:

$$\begin{aligned}
& \rho_b \|\dot{\boldsymbol{\eta}}^{n+1}\|_{\Omega_b}^2 + \|\boldsymbol{\eta}^{n+1}\|_E^2 + c_b \|p_b^{n+1}\|_{\Omega_b} + [\Delta t]\|(k_b^n)^{1/2} \nabla p_b^{n+1}\|_{\Omega_b}^2 + c_p \|p_p^{n+1}\|_{\Omega_p}^2 \\
& + [\Delta t]\|k_p^{1/2} \partial_s p_p^{n+1}\|_{\Omega_p}^2 + \rho_p \|\dot{w}^{n+1}\|_{\omega_p}^2 + \|\Delta w^{n+1}\|_{\omega_p}^2 + \|\mathbf{u}^{n+1}\|_{\Omega_f}^2 \\
& + [\Delta t]\|\mathbf{D}(\mathbf{u}^{n+1})\|_{\Omega_f}^2 + [\Delta t]\|\mathbf{u}^{n+1} \cdot \mathbf{t}\|_{\omega_p}^2 \\
& \lesssim \rho_b \|\dot{\boldsymbol{\eta}}^n\|_{\Omega_b}^2 + \|\boldsymbol{\eta}^n\|_E^2 + c_b \|p_b^n\|_{\Omega_b}^2 + c_p \|p_p^n\|_{\Omega_p}^2 + \rho_p \|\dot{w}^n\|_{\omega_p}^2 + \|\Delta w^n\|_{\omega_p}^2 \\
& + [\Delta t]\|\mathbf{F}_b^{n+1}\|_{\Omega_b}^2 + [\Delta t]\|S^{n+1}\|_{\Omega_b}^2 + [\Delta t]\|\mathbf{f}^{n+1}\|_{\Omega_f}^2.
\end{aligned}$$

This estimate can be rearranged and expressed as follows:

$$\begin{aligned}
& \rho_b \|\dot{\boldsymbol{\eta}}^{n+1}\|_{\Omega_b}^2 + \|\boldsymbol{\eta}^{n+1}\|_E^2 + c_b \|p_b^{n+1}\|_{\Omega_b} + c_p \|p_p^{n+1}\|_{\Omega_p}^2 \\
& + \rho_p \|\dot{w}^{n+1}\|_{\omega_p}^2 + \|\Delta w^{n+1}\|_{\omega_p}^2 + \|\mathbf{u}^{n+1}\|_{\Omega_f}^2 \\
& \lesssim \rho_b \|\dot{\boldsymbol{\eta}}^n\|_{\Omega_b}^2 + \|\boldsymbol{\eta}^n\|_E^2 + c_b \|p_b^n\|_{\Omega_b}^2 + c_p \|p_p^n\|_{\Omega_p}^2 + \rho_p \|\dot{w}^n\|_{\omega_p}^2 + \|\Delta w^n\|_{\omega_p}^2 \\
& + [\Delta t]\|\mathbf{F}_b^{n+1}\|_{\Omega_b}^2 + [\Delta t]\|S^{n+1}\|_{\Omega_b}^2 + [\Delta t]\|\mathbf{f}^{n+1}\|_{\Omega_f}^2 \\
& - [\Delta t]\|k_b^{1/2} \nabla p_b^{n+1}\|_{\Omega_b}^2 - [\Delta t]\|k_p^{1/2} \partial_s p_p^{n+1}\|_{\Omega_p}^2 - [\Delta t]\|\mathbf{D}(\mathbf{u}^{n+1})\|_{\Omega_f}^2 \\
& - [\Delta t]\|\mathbf{u}^{n+1} \cdot \mathbf{t}\|_{\omega_p}^2.
\end{aligned}$$

Inductively, after rearrangement, we obtain

$$\begin{aligned}
(5.15) \quad & \|\dot{\boldsymbol{\eta}}^{N+1}\|_{\Omega_b}^2 + \|\boldsymbol{\eta}^{N+1}\|_E^2 + c_b \|p_b^{N+1}\|_{\Omega_b} + c_p \|p_p^{N+1}\|_{\Omega_p}^2 + \rho_p \|\dot{w}^{N+1}\|_{\omega_p}^2 \\
& + \|\Delta w^{N+1}\|_{\omega_p}^2 + \|\mathbf{u}^{N+1}\|_{\Omega_f}^2 \\
& + \sum_{n=0}^N \left[\|k_b^{1/2} \nabla p_b^{n+1}\|_{\Omega_b}^2 + \|k_p^{1/2} \partial_s p_p^{n+1}\|_{\Omega_p}^2 + \|\mathbf{D}(\mathbf{u}^{n+1})\|_{\Omega_f}^2 + \|\mathbf{u}^{n+1} \cdot \mathbf{t}\|_{\omega_p}^2 \right] [\Delta t] \\
& \lesssim \|\dot{\boldsymbol{\eta}}^0\|_{\Omega_b}^2 + \|\boldsymbol{\eta}^0\|_E^2 + c_b \|p_b^0\|_{\Omega_b}^2 + c_p \|p_p^0\|_{\Omega_p}^2 + \rho_p \|\dot{w}^0\|_{\omega_p}^2 + \|\Delta w^0\|_{\omega_p}^2 \\
& + \sum_{n=0}^N \left[\|\mathbf{F}_b^{n+1}\|_{\Omega_b}^2 + \|S^{n+1}\|_{\Omega_b}^2 + \|\mathbf{f}^{n+1}\|_{\Omega_f}^2 \right] [\Delta t].
\end{aligned}$$

Noting the lower bound on $k_b \geq k_{\min} > 0$ again, we obtain the uniform estimates for the approximate solutions. \square

We will need two more estimates to be able to pass to the limit as $N \rightarrow \infty$ (or, equivalently, as $\Delta t \rightarrow 0$) in the evolution case when we have to deal with the terms $\dot{\boldsymbol{\eta}}^{[N]}$ and $\dot{w}^{[N]}$. In this case we require bounds on $\dot{\boldsymbol{\eta}}^{[N]}$, $\dot{w}^{[N]}$ in the associated dual,

H^{-1} -like spaces. Additionally, we will need an estimate for the time derivative of the fluid content in the associated dual space.

Having established the solution, such estimates will follow immediately from (5.6). More precisely, since some test functions are coupled, we need to consider duals of product spaces to establish these estimates. In particular, consider first taking all test functions in (5.6) zero except for the “inertial test functions” $(\psi, z) \in H_{\#}^1(\Omega_b) \times H_{\#}^2(\omega_p)$ such that $\psi|_{x_3=0} = z\mathbf{e}_3$. Then, dividing (5.6) by $[\Delta t]$, we obtain the following equality for the solution at any t^{n+1} :

$$\begin{aligned} & \rho_b(\ddot{\boldsymbol{\eta}}^{n+1}, \boldsymbol{\psi})_{\Omega_b} + \rho_p(\ddot{w}^{n+1}, z)_{\omega_p} \\ &= (\boldsymbol{\sigma}_b(\boldsymbol{\eta}^{n+1}, p_b^{n+1}), \nabla \boldsymbol{\psi})_{\Omega_b} + (\mathbf{F}_b^{n+1}, \boldsymbol{\psi})_{\Omega_b} \\ & \quad - D(\Delta w^{n+1}, \Delta z)_{\omega_p} - \alpha_p \left(\int_{-h/2}^{h/2} [sp_p^{n+1}] ds, \Delta z \right)_{\omega_p} - \left(p_p^{n+1} \Big|_{s=-h/2}, z \right)_{\omega_p}. \end{aligned}$$

A similar calculation can be done for the fluid content by taking all test functions zero except for the “fluid content test functions” $(q_p, q_b) \in H_{\#}^1(\Omega_b) \times H_{\#}^{0,0,1}$ such that $q_b|_{s=h/2} = q_p$. After integrating the obtained equalities with respect to time from $t^n = n[\Delta t]$ to $t^{n+1} = (n+1)[\Delta t]$, and taking the sum over n , for $n = 0, \dots, N-1$, the estimates in Lemma 5.5 give the following result.

LEMMA 5.6. *Let $\mathcal{V}_{\text{in}} = \{(\boldsymbol{\psi}, z) \in H_{\#}^1(\Omega_b) \times H_{\#}^2(\omega_p) : \boldsymbol{\psi}|_{x_3=0} = z\mathbf{e}_3\}$ and $\mathcal{V}_{\text{fc}} = \{(q_p, q_b) \in H_{\#}^1(\Omega_b) \times H_{\#}^{0,0,1} : q_b|_{s=h/2} = q_p\}$. Then there exists constant C independent of N such that*

$$\begin{aligned} & \left\| (\rho_b \ddot{\boldsymbol{\eta}}^{[N]}, \rho_p \ddot{w}^{[N]}) \right\|_{\mathcal{V}'_{\text{in}}} \leq C, \\ & \left\| (c_b \dot{p}_b^{[N]} + \alpha_b \nabla \cdot \dot{\boldsymbol{\eta}}^{[N]}, c_p \dot{p}_p^{[N]} - \alpha_p \Delta \dot{w}^{[N]}) \right\|_{\mathcal{V}'_{\text{fc}}} \leq C. \end{aligned}$$

5.3. Limit $N \rightarrow \infty$ and recovery of linear weak solution.

5.3.1. Existence. To prove the existence of a weak solution to the linear Stokes–Biot-poroelate fluid-structure interaction problem (2.15)–(2.30), we would like to show that there exist subsequences of approximate solutions

$$\{(\mathbf{u}^{[N]}, w^{[N]}, p_p^{[N]}, \boldsymbol{\eta}^{[N]}, p_b^{[N]})\}_{N \in \mathbb{N}},$$

which converge, as $N \rightarrow \infty$ (or equivalently, as $\Delta t \rightarrow 0$), to a function which satisfies the weak formulation of the continuous problem specified in Definition 1. Since the problem is linear, weak convergence of subsequences of approximate solutions $\{(\mathbf{u}^{[N]}, w^{[N]}, p_p^{[N]}, \boldsymbol{\eta}^{[N]}, p_b^{[N]})\}_{N \in \mathbb{N}}$ is sufficient to pass to the limit in the weak formulations (5.14) satisfied by the approximate functions and recover the weak formulation of the continuous problem, satisfied by the limiting function. Indeed, the uniform bounds presented in Lemmas 5.5 and 5.6 imply existence of subsequences of $\{(\mathbf{u}^{[N]}, w^{[N]}, p_p^{[N]}, \boldsymbol{\eta}^{[N]}, p_b^{[N]})\}_{N \in \mathbb{N}}$, denoted again with

$$\{(\mathbf{u}^{[N]}, w^{[N]}, p_p^{[N]}, \boldsymbol{\eta}^{[N]}, p_b^{[N]})\}_{N \in \mathbb{N}}$$

(with a slight abuse of notation), such that the following weak convergence is true for those subsequences:

$$(5.16) \quad (\mathbf{u}^{[N]}, w^{[N]}, p_p^{[N]}, \boldsymbol{\eta}^{[N]}, p_b^{[N]}) \rightharpoonup (\mathbf{u}, w, p_p, \boldsymbol{\eta}, p_b) \quad \text{weakly in } \mathcal{V}_{\text{sol}}$$

and

$$\begin{aligned} (\rho_b \ddot{\boldsymbol{\eta}}^{[N]}, \rho_p \ddot{w}^{[N]}) &\overset{*}{\rightharpoonup} (\rho_b \ddot{\boldsymbol{\eta}}, \rho_p \ddot{w}) \quad \text{weakly } * \text{ in } \mathcal{V}_{\text{in}}, \\ (c_b \dot{p}_b^{[N]} + \alpha_b \nabla \cdot \dot{\boldsymbol{\eta}}^{[N]}, c_p \dot{p}_p^{[N]} - \alpha_p \Delta \dot{w}^{[N]}) &\overset{*}{\rightharpoonup} (c_b \dot{p}_b + \alpha_b \nabla \cdot \dot{\boldsymbol{\eta}}, c_p \dot{p}_p - \alpha_p \Delta \dot{w}), \\ &\text{weakly } * \text{ in } \mathcal{V}_{\text{fc}}. \end{aligned}$$

This is sufficient to pass to the limit in (5.14) and obtain that the limiting function satisfies the continuous weak formulation (1). This calculation is straightforward. Therefore, the uniform estimates from Lemmas 5.5 and 5.6 imply the following existence result.

THEOREM 5.7. *Let $c_p > 0$ and $\rho_b, \rho_p, c_b, \rho_f \geq 0$, $\alpha_n, \alpha_p, \mu_E, \lambda_E, D, \mu, k_p > 0$, and $T > 0$. Moreover, let the initial data belong to the following spaces: $\mathbf{u} \in L^2(\Omega_f)$, $w \in H_{\#}^2(\omega_p)$, $w_t \in L^2(\omega_p)$, $\boldsymbol{\eta} \in H_{\#}^1(\omega_p)$, $\boldsymbol{\eta}_t \in L^2(\Omega_b)$, $p_b \in L^2(\Omega_b)$, $p_p \in L^2(\Omega_p)$, and let $k_b \in L^\infty(0, T; L^\infty(\Omega_b))$ such that $0 < k_{\min} \leq k_b \leq k_{\max}$. Then there exists a weak solution on $(0, T)$ in the sense of Definition 1.*

5.3.2. Uniqueness. We conclude this section with a brief discussion of the issue of (linear) uniqueness. First, we note that even in the linear case, the uniqueness of solutions is a nontrivial issue—see [16, 47]. This primarily stems from the fact that the energy estimates obtained for the constructed solution above need not apply to a general weak solution. Hence, given two weak solutions, an a priori estimate on the difference is not immediately obtainable via formal estimation as was done on approximate solutions in the construction of our particular weak solution. This issue is two-pronged: first, the hyperbolic nature of the inertial problem (when ρ_b and/or ρ_p nonzero) has challenges associated to justifying velocity multipliers (test functions) $\boldsymbol{\eta}_t$ and w_t , owing to the higher order terms appearing from the Biot structure of the solid dynamics. Second, Biot models with time dependent coefficients (even in the quasi-static case) have issues associated to multiplier analysis in obtaining a priori estimates. The effect of this can be noted, for instance, in [47, pp. 110–117], where abstract implicit evolutions are discussed and “much non-uniqueness” is possible, since “...the stability estimate...was shown to hold for *some* solution, not every solution...”

We provide a lemma that yields uniqueness, assuming that formal test functions $\boldsymbol{\eta}_t$ and w_t are admissible in the sense of the following hypothesis.

Assumption 5. Assume that the function $(\mathbf{u}, w, p_p, \boldsymbol{\eta}, p_b) \in \mathcal{V}_{\text{sol}}$ has the additional property that

$$(5.17) \quad (\rho_b w_{tt} + D \Delta^2 w, w_t)_{\omega_p} = \frac{1}{2} \frac{d}{dt} \left\{ \rho_p \|w_t\|_{L^2(\omega_p)}^2 + D \|\Delta w\|_{L^2(\omega_p)}^2 \right\},$$

$$(5.18) \quad (\rho_p \boldsymbol{\eta}_{tt} + \boldsymbol{\sigma}^E, \boldsymbol{\eta}_t)_{\Omega_p} = \frac{1}{2} \frac{d}{dt} \left\{ \rho_b \|\boldsymbol{\eta}_t\|_{L^2(\Omega_b)}^2 + \|\boldsymbol{\eta}\|_E^2 \right\}.$$

Then, the following uniqueness result holds.

LEMMA 5.8 (uniqueness of weak solutions). *Let $c_p > 0$ and $\rho_b, \rho_p, c_b, \rho_f \geq 0$, $\alpha_b, \alpha_p, \mu_E, \lambda_E, D, \mu, k_p > 0$, and $T > 0$. Moreover, let $k_b \in L^\infty(\Omega_b \times (0, T))$ such that $0 < k_1 \leq k_b \leq k_2$. Suppose further that a weak solution $(\mathbf{u}, w, p_p, \boldsymbol{\eta}, p_b) \in \mathcal{V}_{\text{sol}}$ has the additional property specified in Assumption 5. Then, for the given data, such a solution is unique.*

Proof. The above lemma follows immediately from the formal energy estimates presented in the preceding section applied to the difference of two solutions to the linear problem. \square

Remark 5.3. Note that Assumption 5 holds, for instance, for strong solutions (for instance, if $w \in C^2([0, T]; L^2(\omega_p)) \cap C^1([0, T]; H^2(\omega_p)) \cap C([0, T]; H^4(\omega_p))$, with analogous assumptions for $\boldsymbol{\eta}$). However, it is not at all obvious when, for instance, ρ_p or ρ_b are zero. In full generality, whether or not w_t and $\boldsymbol{\eta}_t$ are valid to test with for a weak solution is certainly a subtle issue.

6. Main result II: Quasistatic nonlinear problem. In this section we consider the nonlinear case where

- the permeability function k_b depends explicitly on $\zeta_b = c_b p_b + \alpha_b \nabla \cdot \boldsymbol{\eta}$, as specified in (2.10);
- the Biot model (2.15) is quasi-static, as specified in Assumption 4, namely, $\rho_b = 0$ in (2.15);
- we allow $\rho_p \geq 0$ in the poroelastic plate equations (2.16).

The main nonlinear existence result is the following.

THEOREM 6.1 (nonlinear existence of weak solutions). *Let $\rho_b = 0$, $c_p > 0$, and $\rho_p, c_b, \rho_f \geq 0$, $\alpha_n, \alpha_p, \mu_E, \lambda_E, D, \mu, k_p > 0$, and $T > 0$. Moreover, let the initial data belong to the following spaces: $\mathbf{u} \in L^2(\Omega_f)$, $w \in H_{\#}^2(\omega_p)$, $w_t \in L^2$, $\boldsymbol{\eta} \in H_{\#}^1(\Omega_b)$, $\eta_t \in L^2(\Omega_b)$, $p_b \in L^2(\Omega_b)$, $p_p \in L^2(\Omega_p)$, and let $k_b(\cdot) \in L^\infty(\mathbb{R})$ such that $0 < k_{\min} \leq k_b \leq k_{\max}$. Then, there exists a weak solution to the nonlinear quasi-static problem on $(0, T)$ in the sense of Definition 1, with $\rho_b = 0$.*

To prove this result, we first notice that all the steps in the existence proof performed for the linear case still hold, except the last step involving passage to the limit. To pass to the limit in the nonlinear problem we will use a version of the Aubin–Lions lemma obtained in [29], which is particularly suitable for piecewise constant approximations in time of the approximate solutions constructed using Rothe’s method. Here we state the special case of [29, Theorem 1] adapted to our notation.

THEOREM 6.2 (compactness Lemma [29]). *Let $V \hookrightarrow H \hookrightarrow W$ be Hilbert spaces with the first inclusion compact and the second continuous. Consider the sequence of piecewise constant in time functions $u^{[N]}$ (indexed by $N \rightarrow \infty$, or equivalently, $[\Delta t] \rightarrow 0$), and $\dot{u}^{[N]}$ defined in (5.13).*

If the following inequality holds,

$$\|\dot{u}^{[N]}\|_{L^2([\Delta t], T; W)} + \|u^{[N]}\|_{L^2(0, T; V)} \leq C$$

with C independent of N , then $u^{[N]}$ is precompact in $L^2(0, T; H)$.

We will apply this theorem on the sequence $[c_b p_b^{[N]} + \alpha_b \nabla \cdot \boldsymbol{\eta}^{[N]}]$ with $W = L^2(0, T; H^{-1}(\Omega_b))$, $V = L^2(0, T; H^e(\Omega_b))$, and $H = L^2(0, T; L^2(\Omega_b))$.

We start by showing the following uniform estimate on $[c_b p_b^{[N]} + \alpha_b \nabla \cdot \dot{\boldsymbol{\eta}}^{[N]}]$.

LEMMA 6.3. *There exists a constant C independent of N such that*

$$\|c_b p_b^{[N]} + \alpha_b \nabla \cdot \dot{\boldsymbol{\eta}}^{[N]}\|_{L^2(0, T; H^{-1}(\Omega_b))} \leq C.$$

Proof. Let $q_b \in C_c^1((0, T); H_0^1(\Omega_b))$. Then $(0, 0, 0, 0, q_b)$ belongs to the space of test functions V_{test} . Therefore we can use this test function in the weak formulation (5.14) for approximate solutions to obtain (due to the second equation in (2.15)):

$$\begin{aligned} ((c_b p_b^{[N]} + \alpha_b \nabla \cdot \dot{\boldsymbol{\eta}}^{[N]}, q_b))_{\Omega_b} \\ = -((k_b(\tau_{\Delta t}(c_b p_b^{[N]} + \alpha_b \nabla \cdot \boldsymbol{\eta}^{[N]})) \nabla p_b^{[N]}, \nabla q_b))_{\Omega_b} + ((S^{[N]}, q_b))_{\Omega_b}. \end{aligned}$$

By using uniform estimates presented in Lemma 5.5, we obtain the following estimate:

$$\begin{aligned} |((c_b p_b^{[N]} + \alpha_b \nabla \cdot \boldsymbol{\eta}^{[N]}, q_b))_{\Omega_b}| &\leq k_{\max} \|\nabla p_b^{[N]}\|_{L_t^2 L_x^2} \|q_b\|_{L_t^2 H_x^1} + C \|S^{[N]}\|_{L_t^2 L_x^2} \|q_b\|_{L_t^2 H_x^1} \\ &\leq C \|q_b\|_{L_t^2 H_x^1}. \end{aligned}$$

Now the conclusion of the lemma follows by density arguments and from the converse of Hölder's inequality. \square

In order to prove the compactness result, we need the regularity result for the Biot displacement.

THEOREM 6.4. *In the quasistatic case ($\rho_b = 0$), the Biot displacement satisfies the following additional regularity property: the sequence $\boldsymbol{\eta}^{[N]}$ is uniformly bounded in $L^2(0, T; \mathbf{H}^2(\Omega_b))$.*

Proof. We use the arguments and notation similar to [14, section 3.3]. We denote by $\mathcal{E} : \mathcal{D}(\mathcal{E}) \subset \mathbf{L}^2(\Omega_b) \rightarrow \mathbf{L}^2(\Omega_b)$ the Lamé operator,

$$\mathcal{E}(\boldsymbol{\eta}) := -\nabla \cdot (2\mu_b \mathbf{D}(\boldsymbol{\eta}) + \lambda_b \nabla \cdot \boldsymbol{\eta} \mathbf{I}),$$

defined on the domain

$$\mathcal{D}(\mathcal{E}) = \{\boldsymbol{\eta} \in \mathbf{H}_{\#}^1(\Omega_b) \mid \nabla \cdot (2\mu_b \mathbf{D}(\boldsymbol{\eta}) + \lambda_b \nabla \cdot \boldsymbol{\eta} \mathbf{I}) \in \mathbf{L}^2(\Omega_b)\}.$$

Then $\boldsymbol{\eta}^{[N]}$ satisfies the following equation:

$$\mathcal{E}\boldsymbol{\eta}^{[N]} = -\nabla p^{[N]} \quad \text{in } (0, T) \times \Omega_b$$

with the following mixed boundary conditions:

1. periodic at $x_i = 0, x_i = 1$ for $i = 1, 2$ (see (2.25));
2. zero traction condition at $x_3 = 1$ (see (2.27));
3. Dirichlet condition on $x_3 = 0$, i.e., on ω_p : $\boldsymbol{\eta}^{[N]} = w^{[N]} \mathbf{e}_3$ (see (2.19)).

From Lemma 5.5 we see that

- the right-hand side ∇p in uniformly bounded in $L^2(0, T; L^2(\Omega_b))$;
- the sequence $w^{[N]}$ in the Dirichlet boundary condition is uniformly bounded in $L^\infty(0, T; H^2(\omega_p))$.

Now the conclusion of the Lemma follows directly from standard elliptic regularity on a rectangular prism, as in [14, Lemma 2]. \square

Remark 6.1. First, it is important to note here that due to the way the problem is set up, our domain is smooth without corners. Second, the full elliptic regularity recovered in Theorem 6.4 is more than is needed in the construction of solutions; indeed, if $\boldsymbol{\eta}^{[N]}$ is uniformly bounded in $L^2(0, T; \mathbf{H}^{1+\epsilon}(\Omega_b))$, $\epsilon > 0$, then the convergence properties stated below follow as in [14].

COROLLARY 6.5. *The following convergence properties hold:*

$$\begin{aligned} c_b p_b^{[N]} + \alpha_b \nabla \cdot \boldsymbol{\eta}^{[N]} &\rightarrow c_b p_b + \alpha_b \nabla \cdot \boldsymbol{\eta} \quad \text{strongly in } L^2(0, T; L^2(\Omega_b)), \\ k_b (\tau_{\Delta t} (c_b p_b^{[N]} + \alpha_b \nabla \cdot \boldsymbol{\eta}^{[N]})) &\rightarrow k_b (c_b p_b + \alpha_b \nabla \cdot \boldsymbol{\eta}) \quad \text{strongly in } L^2(0, T; L^2(\Omega_b)). \end{aligned}$$

Proof. Uniform energy estimates from Lemma 5.5 imply that sequence $p_b^{[N]}$ is uniformly bounded in $L^2(0, T; H^1(\Omega_b))$. Therefore, by Theorem 6.4, sequence $c_b p_b^{[N]} +$

$\alpha_b \nabla \cdot \boldsymbol{\eta}^{[N]}$ is uniformly bounded in $L^2(0, T; H^\epsilon(\Omega_b))$. Moreover, by Lemma 6.3 sequence $(c_b p_b^{[N]} + \alpha_b \nabla \cdot \boldsymbol{\eta}^{[N]})$ is uniformly bounded in $L^2(0, T; H^{-1}(\Omega_b))$.

The strong convergence of $[c_b p_b^{[N]} + \alpha_b \nabla \cdot \boldsymbol{\eta}^{[N]}]$ then follows by direct application of Theorem 6.2.

The second convergence result follows by noticing that $k_b(\cdot) : L^2(\Omega_b) \rightarrow L^2(\Omega_b)$ represents a Nemytskii operator [47]. This follows from the bounds $0 < k_{\min} \leq k_b(s) \leq \kappa_{\max}$ for all $s \in \mathbb{R}$, as well as the continuity of $k_b(\cdot)$. Thus

$$k_b(\tau_{\Delta t}(c_b p_b^{[N]} + \alpha_b \nabla \cdot \boldsymbol{\eta}^{[N]})) \rightarrow k_b(c_b p_b + \alpha_b \nabla \cdot \boldsymbol{\eta}),$$

as desired. \square

To complete the proof of the existence of weak solutions, what remains to show is how to pass to the limit in the nonlinear term in (5.14). For this purpose, we recall the following convergence properties of the sequences appearing in the nonlinear term:

$$k_b(\tau_{\Delta t}(c_b p_b^{[N]} + \alpha_b \nabla \cdot \boldsymbol{\eta}^{[N]})) \rightarrow k_b(c_b p_b + \alpha_b \nabla \cdot \boldsymbol{\eta}) \text{ in } L^2(0, T; L^2(\Omega_b)),$$

$$\nabla p_b^{[N]} \rightharpoonup \nabla p_b \text{ weakly in } L^2(0, T; L^2(\Omega_b)).$$

Now, by the convergence of weak-strong products we get

$$k_b(\tau_{\Delta t}(c_b p_b^{[N]} + \alpha_b \nabla \cdot \boldsymbol{\eta}^{[N]})) \nabla p_b^{[N]} \rightharpoonup k_b(c_b p_b + \alpha_b \nabla \cdot \boldsymbol{\eta}) \nabla p_b \text{ in } L^1(0, T; L^1(\Omega_b)).$$

To see that this sequence converges weakly in $L^2(0, T; L^2(\Omega_b))$, we recall that $k_b(\tau_{\Delta t}(c_b p_b^{[N]} + \alpha_b \nabla \cdot \boldsymbol{\eta}^{[N]})) \nabla p_b^{[N]}$ is a bounded sequence in $L^2(0, T; L^2(\Omega_b))$, and therefore it has a subsequence which converges weakly in $L^2(0, T; L^2(\Omega_b))$. Because of the uniqueness of the limit in \mathcal{D}' , its limit is exactly $k_b(c_b p_b + \alpha_b \nabla \cdot \boldsymbol{\eta}) \nabla p_b$. \square

6.1. Uniqueness. Last, we consider the issue of uniqueness for nonlinear solutions. At present, even for the nonlinear Biot system alone, a full uniqueness result does not exist in the literature. In [22], a *central* hypothesis for the entire well-posedness analysis is that $c_b > 0$; for uniqueness, the permeability function k_b is assumed to be Lipschitz continuous, and a smallness hypothesis is also imposed on the Biot pressure.

Along these lines, we present here a strong-weak uniqueness result for mild solutions. More precisely, in addition to assuming that our weak solutions satisfy an energy-type equality, specified in Assumption 5, which is related to allowing $\boldsymbol{\eta}_t$ to serve as a test function (multiplier), we also require some additional regularity on the Biot pressure, as specified below in Lemma 6.6.

More precisely, we introduce the space

$$\mathcal{W} \subset \mathcal{V}_{\text{sol}} \text{ such that Assumption 5 is satisfied,}$$

and consider solutions in \mathcal{W} with the additional regularity for p_b as follows.

PROPOSITION 6.6 (uniqueness of weak solutions). *Let $c_p > 0$ with $\rho_b = 0$, and $\rho_p, c_b, \rho_f \geq 0$, $\alpha_n, \alpha_p, \mu_E, \lambda_E, D, \mu, k_p > 0$. Moreover, let $k_b \in L^\infty(\mathbb{R}) \cap \text{Lip}(\mathbb{R})$ such that $0 < k_{\min} \leq k_b \leq k_{\max}$. Suppose there is a weak solution $(\mathbf{u}, w, p_p, \boldsymbol{\eta}, p_b) \in \mathcal{W}$ and a time $T^* > 0$ so that the following holds:*

$$\nabla p_b \in L^2(0, T^*; \mathbf{L}^\infty(\Omega_b)).$$

Then, all weak solutions in \mathcal{W} are equal to $(\mathbf{u}, w, p_p, \boldsymbol{\eta}, p_b)$ on any interval $t \in [0, T]$ with $T < T^$.*

Proof. Assume that there are two solutions $\mathbf{s}^i = (\mathbf{u}^i, w^i, p_p^i, \boldsymbol{\eta}^i, p_b^i) \in \mathcal{W}$ for $i = 1, 2$. Under the hypothesis that solutions belong to \mathcal{W} , each solution satisfies the formal energy inequality (3.1). Consider the difference $\bar{\mathbf{s}} = \mathbf{s}^1 - \mathbf{s}^2$ (with the “bar” notation for each coordinate as well) as a weak solution to the *difference* equation with the same data $\mathbf{F}_b, S, F_p, \mathbf{f}$, utilizing (in the appropriate sense) $\bar{\mathbf{s}}$ as a test function. Then, for any $T < T^*$, $\bar{\mathbf{s}}$ satisfies the inequality

$$(6.1) \quad \begin{aligned} \mathcal{E}(\bar{\mathbf{s}}(T)) + \int_0^T \left[2\mu_f \|\mathbf{D}(\bar{\mathbf{u}}(t))\|_{L^2(\Omega_f)}^2 + \beta \|\bar{\mathbf{u}}(t) \cdot \mathbf{t}\|_{L^2(\omega_p)}^2 + \|k_p^{1/2} \partial_s \bar{p}_p(t)\|_{L^2(\Omega_p)}^2 \right] dt \\ \leq \mathcal{E}(\bar{\mathbf{s}}(0)) - \int_0^T ([k_b^1(t) \nabla p_b^1(t) - k_b^2(t) \nabla p_b^2(t)], \nabla [p_b^1(t) - p_b^2(t)])_{\Omega_b} dt, \end{aligned}$$

where we denoted

$$\begin{aligned} \mathcal{E}(\mathbf{s}^i) \equiv \frac{1}{2} \Big(\rho_f \|\mathbf{u}^i\|_{L^2(\Omega_f)}^2 + \rho_p \|w^i\|_{L^2(\omega_p)}^2 + c_p \|p_p^i\|_{L^2(\Omega_p)}^2 \\ + \|\boldsymbol{\eta}^i\|_E^2 + c_b \|p_b^i\|_{L^2(\Omega_b)}^2 + D \|\Delta w^i\|_{L^2(\omega_p)}^2 + \gamma \|w^i\|_{L^2(\omega_p)}^2 \Big) \end{aligned}$$

and

$$k_b^i(t) \equiv k_b(c_b p^i(t) + \alpha_b \nabla \cdot \boldsymbol{\eta}^i(t)).$$

We focus on the nonlinear term with the aim of obtaining an estimate on $\bar{\mathbf{s}}$ through the functional \mathcal{E} . We can rewrite the nonlinear term as

$$(6.2) \quad \begin{aligned} \int_0^T ([k_b^1(t) \nabla p_b^1(t) - k_b^2(t) \nabla p_b^2(t)], \nabla \bar{p}_b)_{\Omega_b} dt \\ = \int_0^T ([k_b^1(t) - k_b^2(t)] \nabla p_b^1(t), \nabla \bar{p}_b(t))_{L^2(\Omega_b)} dt \\ + \int_0^T (k_b^2(t) \nabla \bar{p}_b(t), \nabla \bar{p}_b(t))_{L^2(\Omega_b)} dt, \end{aligned}$$

where we used $\bar{p} = p_b^1 - p_b^2$. Using the lower bound on the permeability function $0 < k_{\min} \leq k_b$ and discarding the additional dissipation terms, we obtain the inequality

$$\mathcal{E}(\bar{\mathbf{s}}(T)) + k_{\min} \int_0^T \|\nabla \bar{p}_b\|_{L^2(\Omega_b)}^2 dt \leq \mathcal{E}(\bar{\mathbf{s}}(0)) - \int_0^T ([k_b^1(t) - k_b^2(t)] \nabla p_b^1(t), \nabla \bar{p}_b(t)) dt.$$

The nonlinear term on the right-hand side can be estimated in two ways, yielding the two cases in this theorem. In both cases we will use the Lipschitz hypothesis on the function k_b . Namely, let $L_k > 0$ be the global Lipschitz constant so that

$$\begin{aligned} |k_b^1(t) - k_b^2(t)| &= |k_b(c_b p_b^1(t) + \alpha_b \nabla \cdot \boldsymbol{\eta}^1(t)) - k_b(c_b p_b^2(t) + \alpha_b \nabla \cdot \boldsymbol{\eta}^2(t))| \\ &\leq L_k |c_b \bar{p}_b(t) + \alpha_b \nabla \cdot \bar{\boldsymbol{\eta}}(t)|. \end{aligned}$$

By the Cauchy–Schwarz inequality, we get

$$\begin{aligned} \int_0^T ([k_b^1(t) - k_b^2(t)] \nabla p_b^1(t), \nabla \bar{p}_b(t)) dt \\ \leq L_k \int_0^T \|\nabla p_b^1\|_{L^\infty(\Omega_b)} \|c_b \bar{p}_b(t) + \alpha_b \nabla \cdot \bar{\boldsymbol{\eta}}(t)\|_{L^2(\Omega_b)} \|\nabla \bar{p}_b\|_{L^2(\Omega_b)} dt. \end{aligned}$$

Now we estimate the right-hand side by using the regularity hypothesis, i.e., $\nabla p_b^1 \in L^2(0, T^*; \mathbb{L}^\infty(\Omega_b))$. Namely, from Young's and triangle inequalities we have the following:

$$\begin{aligned} & \int_0^T ([k_b^1(t) - k_b^2(t)] \nabla p_b^1(t), \nabla \bar{p}_b(t)) dt \\ & \leq \int_0^T L_k \|\nabla p_b^1\|_{L^\infty(\Omega_b)} \|c_b \bar{p}_b + \alpha_b \nabla \cdot \bar{\eta}(t)\|_{L^2(\Omega_b)} \|\nabla \bar{p}_b\|_{L^2(\Omega_b)} dt \\ & \leq \frac{L_k^2}{2\epsilon} \|\nabla p_b^1\|_{L^\infty(0, T; L^\infty(\Omega_b))}^2 \left\{ \int_0^T \|c_b \bar{p}_b\|_{L^2(\Omega_b)}^2 dt + \int_0^T \|\alpha_b \nabla \cdot \bar{\eta}(t)\|_{L^2(\Omega_b)}^2 dt \right\} \\ & \quad + \frac{\epsilon}{2} \int_0^T \|\nabla \bar{p}_b\|_{L^2(\Omega_b)}^2 dt. \end{aligned}$$

Choosing $\epsilon = k_{\min}$ to absorb the pressure term into the left-hand side, and by bounding the elasticity term from above by the full $\|\cdot\|_E$ norm, we have the following estimate:

$$\begin{aligned} & \int_0^T ([k_b^1(t) - k_b^2(t)] \nabla p_b^1(t), \nabla \bar{p}_b(t)) dt \\ & \leq \int_0^T L_k \|\nabla p_b^1\|_{L^\infty(\Omega_b)} \|c_b \bar{p}_b + \alpha_b \nabla \cdot \bar{\eta}(t)\|_{L^2(\Omega_b)} \|\nabla \bar{p}_b\|_{L^2(\Omega_b)} dt \\ & \leq \int_0^T \frac{L_k [c_b + \alpha_b^2]}{2k_{\min}} \|\nabla p_b^1(t)\|_{L^\infty(\Omega_b)}^2 \left\{ c_b \|\bar{p}_b(t)\|_{L^2(\Omega_b)}^2 + \|\bar{\eta}(t)\|_E^2 \right\} dt \\ & \quad + \frac{k_{\min}}{2} \int_0^T \|\nabla \bar{p}_b\|_{L^2(\Omega_b)}^2 dt. \end{aligned}$$

After discarding the dissipation term, we get another Grönwall-type estimate:

$$(6.3) \quad \mathcal{E}(\bar{s}(T)) \leq C \mathcal{E}(\bar{s}(0)) + C \frac{L_k^2 [c_b + \alpha_b^2]}{2k_{\min}} \int_0^T \|\nabla p_b^1(t)\|_{L^\infty(\Omega_b)}^2 \mathcal{E}(\bar{s}(t)) dt.$$

Uniqueness follows by applying the L^2 -version of Grönwall's inequality [28]. \square

We conclude this section by mentioning that in three dimensions, the hypothesis of Proposition 6.6 would be satisfied, for instance, if $p_b^1 \in L^2(0, T; H^{2.5+\epsilon}(\Omega_b))$.

REFERENCES

- [1] I. AMBARTSUMYAN, V.J. ERVIN, T. NGUYEN, AND I. YOTOV, *A nonlinear Stokes-Biot model for the interaction of a non-Newtonian fluid with poroelastic media*, ESAIM Math. Model. Numer. Anal., 53 (2019), pp. 1915–1955.
- [2] I. AMBARTSUMYAN, E. KHATTATOV, I. YOTOV, AND P. ZUNINO, *A Lagrange multiplier method for a Stokes-Biot fluid-poroelastic structure interaction model*, Numer. Math., 140 (2018), pp. 513–553.
- [3] J.-L. AURIAULT, *Poroelastic media*, in Homogenization and Porous Media, Interdiscip. Appl. Math. 6, Springer, New York, 1997, pp. 163–182.
- [4] G. AVALOS, P.G. GERDELI, AND B. MUHA, *Wellposedness, spectral analysis and asymptotic stability of a multilayered heat-wave-wave system*, J. Differential Equations, 269 (2020), pp. 7129–7156.
- [5] S. BADIA, A. QUAINI, AND A. QUARTERONI, *Coupling Biot and Navier–Stokes equations for modelling fluid-poroelastic media interaction*, J. Comput. Phys., 228 (2009), pp. 7986–8014.

- [6] H.T. BANKS, K. BEKELE-MAXWELL, L. BOCIU, M. NOORMAN, AND G. GUIDOBONI, *Sensitivity analysis, in poro-elastic and poro-visco-elastic models with respect to boundary data*, Quart. Appl. Math., 75 (2017), pp. 697–735.
- [7] H.T. BANKS, K. BEKELE-MAXWELL, L. BOCIU, M. NOORMAN, AND G. GUIDOBONI, *Local sensitivity via the complex-step derivative approximation for 1-D poro-elastic and poro-visco-elastic models*, Math. Control Relat. Fields, 9 (2019), pp. 623–642.
- [8] H. BARUCQ, M. MADAUNE-TORT, AND P. SAINT-MACARY, *Theoretical aspects of wave propagation for Biot's consolidation problem*, Monografias del Seminario Matemático García de Galdeano, 31 (2004), pp. 449–458.
- [9] H. BARUCQ, M. MADAUNE-TORT, AND P. SAINT-MACARY, *On nonlinear Biot's consolidation models*, Nonlinear Anal., 63 (2005), pp. e985–e995.
- [10] M.A. BIOT, *General theory of three-dimensional consolidation*, J. Appl. Phys., 12 (1941), pp. 155–164.
- [11] M.A. BIOT, *Theory of elasticity and consolidation for a porous anisotropic solid*, J. Appl. Phys., 26 (1955), pp. 182–185.
- [12] M.A. BIOT, *Theory of stability and consolidation of a porous medium under initial stress*, J. Math. Mech., 12 (1963), pp. 521–541.
- [13] L. BOCIU, L. CASTLE, I. LASIECKA, AND A. TUFFAHA, *Minimizing drag in a moving boundary fluid-elasticity interaction*, Nonlinear Anal., 197 (2020).
- [14] L. BOCIU, G. GUIDOBONI, R. SACCO, AND J. T. WEBSTER, *Analysis of nonlinear poro-elastic and poro-visco-elastic models*, Arch. Ration. Mech. Anal., 222 (2016), pp. 1445–1519.
- [15] L. BOCIU, G. GUIDOBONI, R. SACCO, AND M. VERRI, *On the role of compressibility in poro-viscoelastic models*, Math. Biosci. Eng., 16, pp. 6167–6208 <https://doi.org/10.3934/mbe.2019308>.
- [16] L. BOCIU AND J.T. WEBSTER, *Nonlinear quasi-static poroelasticity*, J. Differential Equations, 296 (2021), pp. 242–278.
- [17] L. BOCIU AND M. NOORMAN, *Poro-visco-elastic models in biomechanics: Sensitivity analysis*, Commun. Appl. Anal., 23 (2019), pp. 61–77.
- [18] M. BUKAČ, I. YOTOV, AND P. ZUNINO, *An operator splitting approach for the interaction between a fluid and a multilayered poroelastic structure*, Numer. Methods Partial Differential Equations, 31 (2015), pp. 1054–1100.
- [19] E. BURMAN AND M.A. FERNÁNDEZ, *An unfitted Nitsche method for incompressible fluid-structure interaction using overlapping meshes*, Comput. Methods Appl. Mech. Engrg., 279 (2014), pp. 497–514.
- [20] S. ČANIC, J. TAMBACA, G. GUIDOBONI, A. MIKELIC, C. J. HARTLEY, AND D. ROSENSTRAUCH, *Modeling viscoelastic behavior of arterial walls and their interaction with pulsatile blood flow*, SIAM J. Appl. Math., 67 (2006), pp. 164–193.
- [21] S. ČANIC, Y. WANG, AND M. BUKAČ, *A next-generation mathematical model for drug-eluting stents*, SIAM J. Appl. Math., 81 (2021), pp. 1503–1529.
- [22] Y. CAO, S. CHEN, AND A.J. MEIR, *Analysis and numerical approximations of equations of nonlinear poroelasticity*, Discrete Contin. Dyn. Syst. Ser. B, 18 (2013), pp. 1253–1273.
- [23] P. CAUSIN, G. GUIDOBONI, A. HARRIS, D. PRADA, R. SACCO, AND SAMUELE TERRAGNI, *A poroelastic model for the perfusion of the lamina cribrosa in the optic nerve head*, Math. Biosci., 257 (2014), pp. 33–41.
- [24] A. CESMELIOGLU, *Analysis of the coupled Navier-Stokes/Biot problem*, J. Math. Anal. Appl., 456 (2017), pp. 970–991.
- [25] O. COUSSY, Poromechanics. John Wiley & Sons, New York, 2004.
- [26] S.C. COWIN, *Bone poroelasticity*, J. Biomech., 32 (1999), pp. 217–238.
- [27] E. DETOURNAY AND A.H.-D. CHENG, *Fundamentals of poroelasticity*, in Analysis and Design Methods, Elsevier, New York, 1993, pp. 113–171.
- [28] S.S. DRAGOMIR, *Some Gronwall Type Inequalities and Applications*, Nova Science, Hauppauge, New York, 2003.
- [29] M. DREHER AND A. JÜNGEL, *Compact families of piecewise constant functions in $L_p(0, T; B)$* , Nonlinear Anal., 75 (2012), pp. 3072–3077.
- [30] J.L. FERRIN AND A. MIKELIĆ, *Homogenizing the acoustic properties of a porous matrix containing an incompressible inviscid fluid*, Math. Methods Appl. Sci., 26 (2003), pp. 831–859.
- [31] Y.C. FUNG, *Foundation of Solid Mechanics*, Prentice-Hall, Englewood Cliffs, New Jersey, 1965.
- [32] J.M. HUYGHE, T. ARTS, D.H. VAN CAMPEN, AND R.S. RENEMAN, *Porous medium finite element model of the beating left ventricle*, Amer. J. Physiology, 262 (1992), pp. 1256–1267.
- [33] C.T. HSU AND P. CHENG, *Thermal dispersion in a porous media*, Int. J. Heat Mass Tran., 33 (1990), pp. 1587–1597.

- [34] W. JÄGER AND A. MIKELIĆ, *On the boundary conditions at the contact interface between a porous medium and a free fluid*, Ann. Sc. Norm. Sup. Pisa Cl. Sci. (4), 23 (1996), pp. 403–465.
- [35] W. JÄGER AND A. MIKELIĆ, *On the interface boundary condition of Beavers, Joseph, and Saffman*, SIAM J. Appl. Math., 60 (2000), pp. 1111–1127.
- [36] A. MARCINIAK-CZOCZRA AND A. MIKELIĆ, *A rigorous derivation of the equations for the clamped Biot-Kirchhoff-Love poroelastic plate*, Arch. Ration. Mech. Anal., 215 (2015), pp. 1035–1062.
- [37] A. MIKELIĆ AND J. TAMBAČA, *Derivation of a poroelastic flexural shell model*, Multiscale Model. Simul., 14 (2016), pp. 364–397.
- [38] A. MIKELIĆ AND M.F. WHEELER, *On the interface law between a deformable porous medium containing a viscous fluid and an elastic body*, Math. Models Methods Appl. Sci., 22 (2012), 1250031, 32.
- [39] B. MUHA, *A note on optimal regularity and regularizing effects of point mass coupling for a heat-wave system*, J. Math. Anal. Appl., 425 (2015), pp. 1134–1147.
- [40] B. MUHA AND S. CANIC, *Existence of a weak solution to a nonlinear fluid-structure interaction problem modeling the flow of an incompressible, viscous fluid in a cylinder with deformable walls*, Arch. Ration. Mech. Anal., 207 (2013), pp. 919–968.
- [41] B. MUHA AND S. CANIC, *Existence of a solution to a fluid-multi-layered-structure interaction problem*, J. Differential Equations, 256 (2014), pp. 658–706.
- [42] J. NITSCHKE, *Über ein Variationsprinzip zur Lösung von Dirichlet-Problemen bei Verwendung von Teilräumen, die keinen Randbedingungen unterworfen sind*, Abhandlungen aus dem mathematischen Seminar der Universität Hamburg, 36 (1971), pp. 9–15.
- [43] S. OWCZAREK, *A Galerkin method for Biot consolidation model*, Math. Mech. Solids, 15 (2010), pp. 42–56.
- [44] M. RENARDY AND R.C. ROGERS, *An Introduction to Partial Differential Equations*, Springer, New York, 1992.
- [45] E. ROHAN AND V. LUKEŠ, *Homogenization of the vibro-acoustic transmission on perforated plates*, Appl. Math. Comput., (2019), pp. 821–845.
- [46] E. ROHAN AND S. NAILI, *Homogenization of the fluid-structure interaction in acoustics of porous media perfused by viscous fluid*, Z. Angew. Math. Phys., 71 (2020).
- [47] R.E. SHOWALTER, *Monotone Operators in Banach Space and Nonlinear Partial Differential Equations*, Math. Surveys Monogr. 49, AMS, Providence, RI, 1996.
- [48] R.E. SHOWALTER, *Poroelastic filtration coupled to Stokes flow*, in Control Theory of Partial Differential Equations, Lect. Notes Pure Appl. Math. 242, Chapman & Hall/CRC, Boca Raton, FL, 2005, pp. 229–241.
- [49] R.E. SHOWALTER, *Diffusion in poroelastic media*, J. Math. Anal. Appl., 251 (2000), pp. 310–340.
- [50] S. SONG, G. FALEO, R. YEUNG, R. KANT, A.M. POSSELT, T.A. DESAI, Q. TANG, AND S. ROY, *Silicon nanopore membrane (SNM) for islet encapsulation and immunoisolation under convective transport*, Sci. Rep., 6 (2016), pp. 1–9.
- [51] N. SU AND R.E. SHOWALTER, *Partially saturated flow in a poroelastic medium*, Discrete Contin. Dyn. Syst. Ser. B, 1 (2001), pp. 403–420.
- [52] F. TROLTZSCH, *Optimal Control of Partial Differential Equations—Theory, Methods and Applications*, AMS, Providence, RI, 2010.
- [53] M. VERRI, G. GUIDOBONI, L. BOCIU, AND R. SACCO, *The role of structural viscoelasticity in deformable porous media with incompressible constituents: Applications in biomechanics*, Math. Biosci. Eng., 15 (2018), pp. 933–959.
- [54] A. ZENISEK, *The existence and uniqueness theorem in Biot’s consolidation theory*, Appl. Math., 29 (1984), pp. 194–211.